IEEE Access
Multidisciplinary | Rapid Review | Open Access Journal

Received January 30, 2020, accepted February 20, 2020, date of publication March 5, 2020, date of current version March 30, 2020.

Digital Object Identifier 10.1109/ACCESS.2020.2978495

Localization Based on Probabilistic Multilateration Approach for Mobile Wireless Sensor Networks

JOAQUIN MASS-SANCHEZ[1], CESAR VARGAS-ROSALES[2], (Senior Member, IEEE), ERICA RUIZ-IBARRA[1], ARMANDO GARCIA-BERUMEN[1], AND ADOLFO ESPINOZA-RUIZ[1]

[1]Electrical Engineering Department, Sonora Institute of Technology, Obregon 85130, Mexico
[2]Escuela de Ingenieria y Ciencias, Tecnológico de Monterrey, Monterrey 64849, Mexico

Corresponding author: Erica Ruiz-Ibarra (erica.ruiz@itson.edu.mx)

This work was supported by Programa de Fortalecimiento de la Calidad Educativa (PFCE) 2019.

ABSTRACT Localization is one of the main problems in Mobile Wireless Sensor Networks, since it provides the location of an event occurrence. This paper presents a performance evaluation of the localization algorithms: Multilateration Algorithm, Weighted Multilateration Algorithm and Probabilistic Multilateration Algorithm (PMA). In addition, we propose an Improved Probabilistic Multilateration Algorithm that decreases the localization error of the interest node by using an approach that computes iteratively the position of a node of interest until it reaches the solution that minimizes the localization error. The proposed approach regards the noisy environment by its impact on a correlation matrix that involves the variance of the separation distance between the node of interest and the respective reference nodes (RNs). Furthermore, we also introduce a constant parameter called damping factor; which enhances the convergence of the localization algorithm providing the solution that minimizes the localization error. In this study, we evaluate localization algorithms in a single-hop and multi-hop scenarios considering a distribution with solid geometry of the RNs and randomly distributed RNs in both scenarios. The results we obtained show that our proposed algorithm Improved PMA presents a better performance according to the Normalized Root Mean Squared Error varying the number of reference nodes and noise proportion.

INDEX TERMS MWSNs, reference nodes, NOI, reconfigurable network, ad-hoc networks, localization, mobility patterns.

I. INTRODUCTION

Nowadays, the Mobile Wireless Sensor Networks (MWSNs) play a fundamental role in the communication networks [1], since they are used in many applications, such as tracking [2], [3], real-time localization [4], [5], search and preservation of natural resources [6], power consumption systems [7], Internet of the Things (IoT) [8], physical environments monitoring [5], [9]–[12], traffic monitoring [13], industry and agriculture [6], health care [5], natural disaster prevention [12], etc. MWSNs are composed of nodes spatially distributed over a geographic area of interest; where nodes are equipped into vehicles or mobile robots that move in certain environment [14]. Generally, such devices consist of low consumption proccesors, low processing capacity, low cost; some of their tasks include data collection, processing and transmission of information and cooperation with other nodes [1], [4], [15].

Localization is one of the main problems in WSN, since it provides useful information about an event ocurrence. Localization information is useful for a large number of applications such as routing [3], [5], [15], health surveillance [1], [5], battle field surveillance [5], [9]–[11], underwater environments [16], target tracking [1], [3], logistics, power consumption [7], spatial querying [3], load balancing [17], rescue operations [5], [18], [19], etc. In a reconfigurable network, all the collected information by a single node is transmitted by multiple nodes (through the use of multiple hops) until the access point is reached [20], [21]. In ad-hoc networks, the nodes in between the Node of Interest (NOI) and the

The associate editor coordinating the review of this manuscript and approving it for publication was Muhammad Omer Farooq.

Reference Nodes (RNs) can help determine the position of the NOI in the network [20], [21]. The RNs are nodes whose position is known, and we can achieve this by either equipping them with a Global Positioning System (GPS) device or distributing them in strategic zones with a known location. GPS is a technology able to estimate the position of a mobile device on a particular geographic area; but due to the system higher costs, higher power consumption and inefficiency in indoor environments, it is not the best fit [22]. In addition to the GPS issue, cell phone and WiFi systems do not perform well in certain scenarios such as highlands, underground and disaster zones where the satellite signals or signals from the mobile infrastructure cannot be received [23].

At present, there is a great variety of localization algorithms that do not consider environments with mobile nodes. In localization with static nodes, the NOI is located only once. In contrast, in an MWSN the NOI is continuously localized due to the mobility of the itself [24]. The mobility of the node in a MWSN implies a greater energy consumption, shorter lifetime of the node and increased communication cost [24]. Some advantages of the MWSNs over a WSN with static nodes are greater coverage in the network, greater number of neighboring nodes of the NOI, better network security and increased network connectivity [24]. In MWSN, there are three mobility scenarios [24], [25]: (1) Static RNs and moving sensor nodes, (2) static sensor nodes and moving RNs and (3) moving RNs and moving sensor nodes.

This study uses the first mobility scenario; where we assume that the RNs are static and their positions are known; additionally it is considered that the localization of the sensor nodes will be done only once. The performance of the range-based algorithms is evaluated in this scenario; algorithms such as Multilateration Algorithm (MA), Weighted Multilateration Algorithm (WMA) and Probabilistic Multilateration Algorithm (PMA). The Improved Probabilistic Multilateration Algorithm is also introduced as an improvement of the PMA approach. The Improved PMA algorithm resolves the localization problem iteratively until it gets the position of the NOI that minimizes the localization error. We utilize the Received Signal Strength (RSS) in order to estimate the separation distance between the NOI and the RNs. Besides, we consider that the estimated separation distance between the NOI and the RNs is affected by a random variable with beta distribution due to the mobility of the NOI; which is obtained through several simulations of the NOI motion varying the speed and the direction of it in different instants of time. The localization algorithms analyzed in this paper are evaluated in a single-hop scenario and multi-hop scenario considering different distributions of the RNs, namely, a scenario with fixed RNs distributed on a solid geometry and a scenario with randomly distributed RNs. The performance of the localizations algorithms analyzed in this work is obtained according to the performance metric Normalized Root Mean Squared Error (RMSE). The results we obtained show that our proposed algorithm Improved PMA presents a better performance according to the Normalized RMSE in all the proposed scenarios.

The rest of the paper is structured as follows: Section II presents the work related to the mobility patterns and classification of localization algorithms in MWSNs; Section III describes the localization problem in a network with mobile nodes; Section IV presents the performance analysis of localization techniques MA, WMA and PMA analyzed in this paper; Section V introduces the analysis of the algorithm, which we propose, Improved PMA; Section VI presents the results of the localization algorithms analyzed in this work and finally we present the conclusions that support this study.

II. RELATED WORK

Nowadays MSNSs are considered in large-scale applications; which consist in a great number of sensor nodes and sinks wirelessly connected through an arbitrary topology [1]. Therefore, mobility plays an important role in MWSNs and it can be applied in all the sensors of the MWSN depending on the application [1], [3]. Mobility in a MWSN is divided into three categories: random mobility, predictable mobility and controlled mobility [3]. In the random mobility category, mobile devices move freely and randomly over an interest area with no constraint. In the second category, the trajectory of the mobile device is known and cannot be altered. In the third category related to controlled mobility, the mobile device moves to a known destination following a mobility pattern for a common aim, usually exploration and localization. Nowadays there are many proposals in regards to mobility models that predict the motion of a sensor node [3]. In MWSNs, mobility models predict the trajectory of a moving sensor node [1], [26]. Mobility models describe the speed changes, acceleration and position of a sensor node with respect to time; and they are often used to investigate new propositions on communication and navigation techniques.

Mobility patterns are classified in: trace models and syntactic models [1], [27]. Trace models are mobility deterministic patterns that can be observed in real life. In WNS, trace models cannot be modeled if the traces have not been formed. Therefore, in ad-hoc networks it is necessary to use syntactic models to describe the mobility pattern of the sensor node. Syntactic models describe the realistic movement of a sensor node without considering traces. Syntactic models are classified in entity models and group mobility models [1], [27]. According to the specific features of the syntactic models; these can be classified in random models, time-dependence models, spatial-dependence models and models with geographic constraints. Some mobility patterns based on entity mobility are: random way point, random walk, random Gauss-Markov, city section, random direction, boundless simulation area and the probabilistic version of random walk [1], [28]. The mobility models based on group mobility models are the Exponential Correlated Random, Reference Point Group Mobility (RPGM), Column Mobility Model, Nomadic Community, Pursue Mobility Model, Drift Group and Group Force [1], [28].

In MWSNs, localization algorithms are classified in two: range-free and range-based [29], [30]. The range-based algorithms estimate the separation distance between the RNs and the NOI by means of a technique to estimate distance, such as Time of Arrival (ToA), Received Signal Strength (RSS), Time Difference of Arrival (TDoA) or Angle of Arrival (AoA) [21]. The range-free algorithms use the connectivity information between the nodes to estimate the separation distance between two nodes [21], [31]. The range-based algorithms reach a higher accuracy in the localization of the NOI than the range-free algorithms; but these require extra hardware in the NOI estimation [21], [31]. In many studies, the RSS is used to estimate the distance between the RNs and the NOI; since this technique can be easily implemented in hardware, but its accuracy in the NOI localization is lower than that when the ToA, TDoA and AoA techniques are used, [21], [32]. ToA presents the syncing nodes issue, TDoA has limited coverage and AoA implies computationally expensive hardware and it also requires an antenna array [21].

Some range-free localization algorithms are the centroid [21], weighted centroid [21], Approximate Point In Triangle (APIT) [33], [34], Distance Vector-Hop (DV-Hop) [31], Improved DV-Hop (IDV-Hop) [31], Weighted DV-Hop (WDV-Hop) [31]; circular, rectangular and hexagonal intersection respectively [35], inter alia. In MWSNs; several range-free localization algorithms use the sequential method Monte Carlos (SMC) to estimate the position of the NOI [24], [36]. The Monte Carlo method uses the probability density function (pdf) to estimate the position of the NOI. This method performs the estimation of the NOI in three stages: initialization, sampling and filtering [36]. In the initialization phase, the NOI estimates its localization by generating a set of samples randomly distributed within the sensing area. During the sampling phase, the NOI generates new samples of the coordinates based on the coordinates received on a previous time interval. In this phase, the NOI uses the pdf to generate new randomly distributed samples. Finally, in the filtering phase, the samples from one or two hops of the RNs are used in order to estimate the position of the NOI. In [12], [37], authors propose the algorithm Weighted Monte Carlos Localization (WMCL), which is based on the method SMC [36]. This proposal improves the accuracy on the localization of the NOI in comparison with the DV-Hop [31] and SMC [36]. The method WMCL reduces the sampling area where the NOI is found, by using the bounded box method [36] and it improves the efficiency localization of the SMC method by using the position information of the neighboring nodes of the RNs. The hop distance method uses the average distance per hop between two RNs to estimate the position of the NOI [36]. The Hop distance approach determines the position of the NOI in three phases, namely, localization broadcast, distance matrix calculation and localization estimation [36]. The disvantage of hop distance method is that it requires the RNs to be evenly distributed in the network to achieve high accuracy in the estimation of the position of the NOI. In [36], authors propose the fingerprint approach, which estimates the position of the NOI through two phases, namely, offline and online stage.

Within the literature related to range-based algorithms we can mention DV-Distance [38], Multilateration [39], Multidimensional-Scaling (MDS) [40], Hyperbolic Positioning Algorithm [21], Weighted Hyperbolic Positioning Algorithm [21], [31], Circular and Weighted Circular Positioning Algorithm [21] Weighted Least-Squares (WLS) Multilateration [21], Least-Squares DV-Hop (LSDV-Hop) [41], Vertex Projection [20], Vertex Projection with Correcting Factor and Maximum Likelihood [20]. In MWSNs Bergamo and Mazzini [42] propose a range-based algorithm that uses the information of the positions of the RNs placed on two corners of the same side of a rectangular space. The mobile NOI measures the RSS of the RNs and estimates its position through triangulation. The localization accuracy of this algorithm is affected by the fading away of the signals and mobility of the NOI. Due to the RNs remaining static, the localization of the mobile NOI is limited; given that the RSS decreases as the NOI distances itself from its respective RNs. Therefore, the results of the distance estimated between the mobile NOI and its respective RNs are vague [42]. In [24], authors propose the Dead Reckoning algorithm, which performs the estimation of the position of the NOI in discrete time intervals called checkpoints. The Dead Reckoning carries out the estimation of the NOI localization in two stages: initialization and sequent. In the initialization phase, the NOI is localized by means of trilateration. In the next phase, only two RNs are used to localize the NOI. In this phase, two possible NOI localizations are obtained through the Bézout's theorem [43].

Also in [24], authors propose two classes of localization algorithms for MWSNs: adaptive and predictive. The adaptive localization algorithms carry out the localization of the NOI at constant time intervals based on the NOI movement; where the estimation of the current position of the NOI is obtained from previous estimations. This method allows the NOI to increase its localization frequency when it moves rapidly, or reduce its localization frequency when its movement is sluggish. The predictive algorithms, estimate the movement pattern of the NOI and predict the future movement of the NOI. The main aim of this method is to consider the frequency of the localization of the NOI instead of the localization algorithm.

III. MODEL DESCRIPTION

This section describes the localization scenario in MWSNs, where it is assumed that the RNs are static with known positions and the NOI is moving. In this scenario, localization is described based on a reference coordinate system, defined by RNs, and sensors nodes whose positions are unknown and will be determined by applying a localization algorithm. Figure 1(a) shows the mobility scenario in a WSN of the NOI identified as node $\mathbf{Z}$ with coordinates (x_τ, y_τ) in a discrete instant of time $\tau = 0, 1, 2, \ldots, t$, with respect to the RN $\mathbf{A}_0$ with known position (x_A, y_A). In this scenario, the NOI

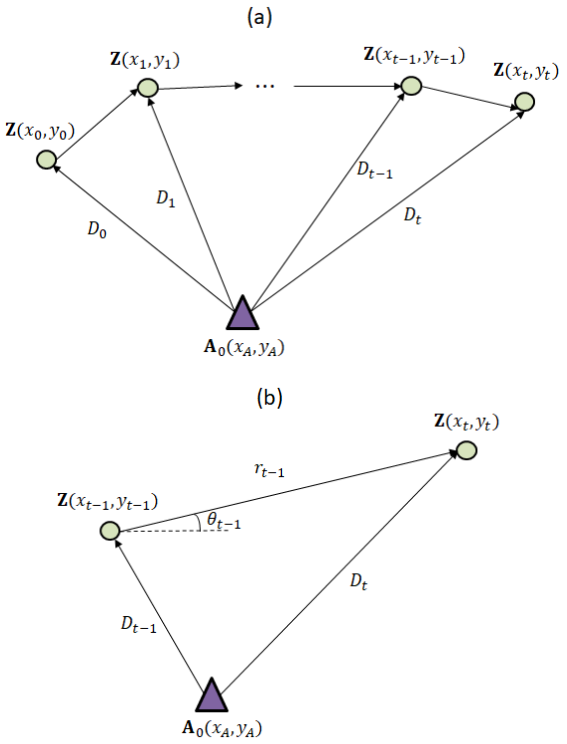

FIGURE 1. Mobility of the NOI Z with respect to the RN $\mathbf{A}_0$.

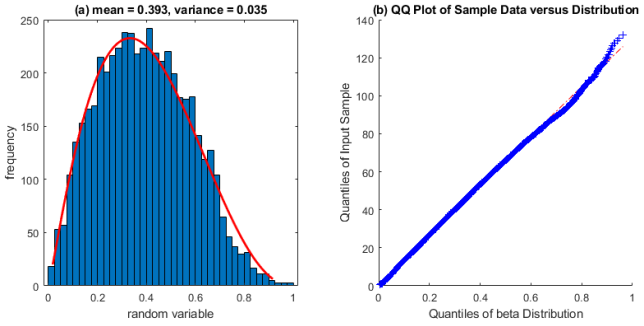

FIGURE 2. (a) pdf of D_t and (b) Q-Q plot beta for $V_{max} = 3$m/s.

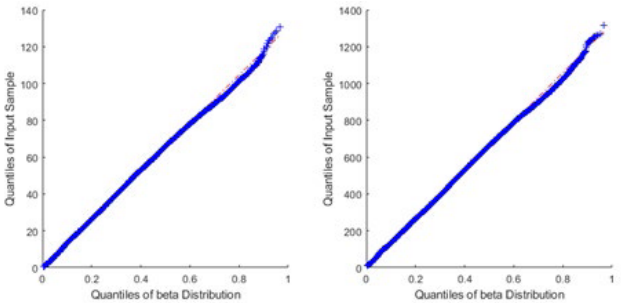

FIGURE 3. Q-Q plot beta for (a) $V_{max} = 5$m/s and (b) $V_{max} = 10$m/s.

$\mathbf{Z}$ motion is based on the random way point mobility pattern. Figure 1(b) shows the transition of the NOI $\mathbf{Z}$ from the instant of time t-1 to the instant of time t, where we obtain a mathematical model of the separation range D_t between the RN $\mathbf{A}_0$ and the mobile NOI $\mathbf{Z}$ in an instant of time t. The elapsed distance r_{t-1} by the NOI $\mathbf{Z}$ is obtained by $r_{t-1} = v_{t-1}\Delta T_{t-1}$, where $v_{t-1} \sim \mathrm{U}(0, V_{max})$, i.e., uniformly distributed in the range $(0, V_{max})$ and ΔT_{t-1} is the time elapsed from the instant of time t-1 to the instant of time t.

The separation distance D_t in the instant of time t between the RN $\mathbf{A}_0$ and the mobile NOI $\mathbf{Z}$ is given by

$$D_t = \sqrt{[x_A - x_t]^2 + [y_A - y_t]^2}. \tag{1}$$

Replacing the motion equations $x_t = x_{t-1} + r_{t-1}\cos(\theta_{t-1})$ and $y_t = y_{t-1} + r_{t-1}\sin(\theta_{t-1})$ of the mobile NOI $\mathbf{Z}$, where $\theta_{t-1} \sim \mathrm{U}(0, 2\pi)$; the separation range D_t is given by

$$D_t = \sqrt{\begin{matrix}\left[x_A - x_{t-1} - v_{t-1}\Delta T_{t-1}\cos(\theta_{t-1})\right]^2 \\ + \left[y_A - y_{t-1} - v_{t-1}\Delta T_{t-1}\sin(\theta_{t-1})\right]^2\end{matrix}}. \tag{2}$$

Note that D_t depends on two random variables, i.e., the speed $v_{t-1} \sim \mathrm{U}(0, V_{max})$ and the direction $\theta_{t-1} \sim \mathrm{U}(0, 2\pi)$, which are asummed to be independent. Since it is not possible to obtain accurate statistical parameters of the variable D_t, we carried out several simulations of the NOI $\mathbf{Z}$ motion with respect to the RN $\mathbf{A}_0$, considering that NOI $\mathbf{Z}$ is moving at different speeds. The results in Figures 2 and 3 show an approximation of the pdf of the separation distance D_t.

Figure 2(a) shows the pdf of the parameter D_t normalized with respect to the maximum possible separation distance between two nodes over an area of 100 m x 100 m, that is 141.42 m, and the pdf of a beta distribution using a red curve, where we may conclude that both pdfs are very similar. In other tests, where the parameter D_t is not normalized we also get a pdf of such parameter very similar to the beta pdf. Figure 2(b) shows a Q-Q (Quantile-Quantile) beta plot, where the calculated pdf is similar to a beta distribution. Similar results are shown in Figure 3 for maximum speeds of the mobile NOI $\mathbf{Z}$ of 5m/s and 10m/s. Therefore, we may conclude that the magnitude of the speed of the mobile NOI $\mathbf{Z}$ does not alter the shape of the pdf of the separation distance D_t, since the results we obtained show that the pdf of the parameter D_t for different speeds is similar to a beta distribution.

Therefore, in a mobility scenario, we assume that the individual distance between the NOI $\mathbf{Z}$ and each one of the RNs (necessary to estimate the position of the NOI $\mathbf{Z}$) has a beta distribution with parameters α and β, i.e., $D_t \sim Beta(\alpha, \beta)$, where D_t is normalized with respect to the maximum possible separation distance between the NOI $\mathbf{Z}$ and the RN $\mathbf{A}_0$, which is 141.42 m over an area of 100 m x 100 m. The parameters α and β define the shape of the pdf with beta distribution. In the simulations performed, in order to obtain the pdf with beta distribution as the speed of the NOI is varied, one can observe that the pdf with beta distribution is similar in all the scenarios. Using parameters α and β, we can estimate distance between the NOI and the RNs, which depends on the speed and the direction of the NOI. By definition the pdf

of a Beta distribution function, is given by

$$f_X(x) = \frac{1}{\mathrm{B}(\alpha,\beta)} x^{\alpha-1}(1-x)^{\beta-1}, \quad 0 < x < 1, \tag{3}$$

where $\mathrm{B}(\alpha,\beta) = \int_0^1 x^{\alpha-1}(1-x)^{\beta-1}dx$. By getting the parameters α and β, we can determine the mean and variance of a random variable X through the following equations

$$\mathrm{E}[X] = \frac{\alpha}{\alpha+\beta}, \tag{4}$$

$$\mathrm{Var}[X] = \frac{\alpha\beta}{(\alpha+\beta)^2(\alpha+\beta+1)}. \tag{5}$$

Assuming the random variable X with beta distribution is defined over a range $0 < x < x_m$, then its pdf is defined by the equation

$$f_X(x) = \frac{1}{x_m \mathrm{B}(\alpha,\beta)} \left(\frac{x}{x_m}\right)^{\alpha-1} \left(1-\frac{x}{x_m}\right)^{\beta-1}, \quad 0 < x < x_m. \tag{6}$$

Therefore, the mean and variance of the random variable X with beta distribution are determined by

$$\mathrm{E}[X] = \frac{\alpha x_m}{\alpha+\beta}, \tag{7}$$

$$\mathrm{Var}[X] = \frac{\alpha\beta x_m}{(\alpha+\beta)^2(\alpha+\beta+1)}. \tag{8}$$

Finally, equations (7)-(8) determine the mean and variance weighted by a factor x_m of a random variable X with beta distribution.

We observe that in an instant of time $\tau = t$, the pdf of the separation distance D_t between the RN $\mathbf{A}_0$ and the NOI $\mathbf{Z}$ has a pdf of a beta distribution with parameters α and β. Thus, it is not necessary to know the parameters of speed v_{t-1}, direction θ_{t-1} and the elapsed time ΔT_{t-1} of the NOI $\mathbf{Z}$ to estimate the separation distance D_t between the RN $\mathbf{A}_0$ and the NOI $\mathbf{Z}$, as we see in equation (2); since these parameters were used to estimate the pdf of a beta distribution with constant parameters α and β. Therefore, the localization of the NOI $\mathbf{Z}$ in the instant of time $\tau = t$, does not depend on previous instants of time, i.e., $\tau = 0, 1, 2, \ldots, t-1$. Without loss of generality, the position of the NOI $\mathbf{Z}$ in an instant of time t is given by the coordinates (x, y).

We consider a network with 3 RNs labeled as $\mathbf{A}_0, \mathbf{B}_0$ and $\mathbf{C}_0$ with known coordinates (x_A, y_A), (x_B, y_B) and (x_C, y_C) respectively, and the NOI $\mathbf{Z}$ with coordinates (x, y) as shown in Figure 4. Assuming that we know the Euclidean ranges $d(\mathbf{A}_0, \mathbf{Z})$, $d(\mathbf{B}_0, \mathbf{Z})$ and $d(\mathbf{C}_0, \mathbf{Z})$ between the NOI $\mathbf{Z}$ and the respective RNs, we can estimate the position of NOI $\mathbf{Z}$ through trilateration. However, due to the limitations of the network coverage, a single node does not provide enough power to achieve a direct link with all the nodes in the network; i.e., the route between the RNs and the NOI $\mathbf{Z}$ is formed by an array of hops in the network. The route from the RN $\mathbf{A}_0$ and the NOI $\mathbf{Z}$ consists of $(1 + n_A)$ nodes, where n_A is the number of hops in such path from the RN $\mathbf{A}_0$ to the NOI $\mathbf{Z}$ (Figure 4). Then, the route from the RN

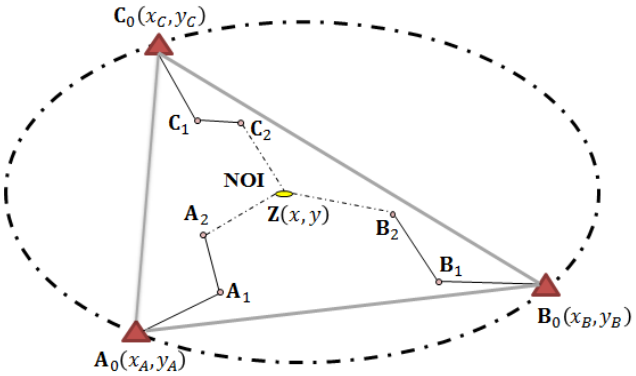

FIGURE 4. Localization scenario with 3 RNs.

$\mathbf{A}_0$ to the NOI $\mathbf{Z}$ is formed by the array of nodes $R_{AZ} = \{\mathbf{A}_0, \mathbf{A}_1, \mathbf{A}_2, \ldots, \mathbf{A}_{n_A-1}, \mathbf{Z}\}$; where $\mathbf{A}_1, \mathbf{A}_2, \ldots, \mathbf{A}_{n_A-1}$ are the intermediate nodes of the route traced from the RN $\mathbf{A}_0$ and the NOI $\mathbf{Z}$. Therefore, the Euclidean range $d(\mathbf{A}_0, \mathbf{Z})$ is formed by the concatenation of multiple hops of length $d(\mathbf{A}_{j-1}, \mathbf{A}_j)$ for $j = 2, 3, \ldots, n_A - 1$; where $\mathbf{A}_j$ is the intermediate node in the path from the RN $\mathbf{A}_0$ to the NOI $\mathbf{Z}$. In a real scenario, the range $d(\mathbf{A}_{j-1}, \mathbf{A}_j)$ for every j can be estimated by using RSS [21].

The log-normal model is used in order to estimate the RSS between two adjacent nodes. This model establishes that the RSS is inversely proportional to the separation distance $d^{-\eta}$; where η is the path-loss exponent [44]. The strength of the received signal $P_r(d)$ with path-loss effects is expressed by

$$P_r(d) = P_T K d^{-\eta} \tag{9}$$

where P_T is the transmitting power, K is a constant factor of path-loss (antenna gains, average channel attenuation, etc.), and d is the separation distance between two nodes. The parameter $P_r(d)$ given in (9), can be expressed in dB assuming path-loss and shadowing effects through

$$P_r(d)_{dB} = (P_T)_{dB} + K_{dB} - 10\eta \log(d) - \chi_\sigma \tag{10}$$

where χ_σ is a random variable with normal distribution with zero mean and standard deviation σ in dB due to shadowing effects, i.e., $\chi_\sigma \sim \mathcal{N}(0, \sigma)$ [44]. The typical values of the path-loss exponent η are in the range of 1.5 to 5 and for the standard deviation σ are in the range of 4 to 12 dB [44]. Equation (10) indicates that RSS value decreases logarithmically with respect to the increasing of the separation distance between the transmitter and receiver. Therefore, by using equation (10), we get the average estimated separation distance $\tilde{\delta}$ given by

$$\tilde{\delta} = 10^{\frac{(P_T)_{dB} + K_{dB} - P_r(d)_{dB}}{10\eta}} \tag{11}$$

As seen in (11), we get the pdf of the separation distance $\tilde{\delta}$, using the following process

$$\begin{aligned} \tilde{\delta} &= 10^{\frac{10\eta\log(d)+\chi_\sigma}{10\eta}} = d\,10^{\left(\frac{\chi_\sigma}{10\eta}\right)} = e^{\ln(d)} 10^{\frac{\chi_\sigma}{10\eta}} \\ &= e^{\ln(d)} e^{\frac{\chi_\sigma \ln(10)}{10\eta}} \\ \tilde{\delta} &= e^{\ln(d) + \frac{\chi_\sigma \ln(10)}{10\eta}} \end{aligned} \tag{12}$$

Equation (12) shows that the term $Y = \ln(d) + \frac{\chi_\sigma \ln(10)}{10\eta}$ is a random variable, since $\chi_\sigma \sim \mathcal{N}(0, \sigma)$. Thus, we may conclude that $Y \sim \mathcal{N}(m_Y, \sigma_Y)$. Then, we get the statistical parameters (m_Y, σ_Y) of the random variable Y as follows

$$m_Y = \mathrm{E}(Y) = \mathrm{E}(\ln(d)) + \mathrm{E}\left(\frac{\chi_\sigma \ln(10)}{10\eta}\right) = \mathrm{E}(\ln(d)) + \frac{\ln(10)}{10\eta}\mathrm{E}(\chi_\sigma) = \ln(d) \quad (13)$$

where $\mathrm{E}(\chi_\sigma) = 0$, since $\chi_\sigma \sim \mathcal{N}(0, \sigma)$. The variance of the Gaussian random variable χ_σ is obtained through $\sigma^2 = \mathrm{E}\left(\chi_\sigma^2\right) - \mathrm{E}^2(\chi_\sigma) = \mathrm{E}\left(\chi_\sigma^2\right)$. The parameter σ_Y is obtained through the following process

$$\sigma_Y^2 = \mathrm{Var}(Y) = \mathrm{E}\left(Y^2\right) - \mathrm{E}^2(Y) = \mathrm{E}\left[\left(\ln(d) + \frac{\chi_\sigma \ln(10)}{10\eta}\right)^2\right] - \ln^2(d) \quad (14)$$

$$\sigma_Y^2 = \mathrm{E}\left[\ln^2(d) + \frac{2\chi_\sigma \ln(d)\ln(10)}{10\eta} + \left(\frac{\chi_\sigma \ln(10)}{10\eta}\right)^2\right] - \ln^2(d)$$

$$\sigma_Y^2 = \mathrm{E}\left[\ln^2(d)\right] + \frac{2\ln(d)\ln(10)}{10\eta}\mathrm{E}(\chi_\sigma) + \left(\frac{\ln(10)}{10\eta}\right)^2 \mathrm{E}\left(\chi_\sigma^2\right) - \ln^2(d)$$

$$\sigma_Y^2 = \ln^2(d) + \left(\frac{\ln(10)}{10\eta}\right)^2 \sigma^2 - \ln^2(d)$$

$$\sigma_Y^2 = \left(\frac{\sigma ln(10)}{10\eta}\right)^2 \quad (15)$$

Therefore, $\sigma_Y = \sigma\ln(10)/10\eta$. Then, $Y \sim \mathcal{N}(m_Y, \sigma_Y)$, where the statistical parameters are given by $m_Y = \ln(d)$ and $\sigma_Y = \sigma\ln(10)/10\eta$. Equation (12) indicates that the estimated separation distance between two nodes has a pdf with log-normal distribution with parameters $\mu_d = \ln(d)$ and $\sigma_d = \sigma\ln(10)/10\eta$, i.e., $\tilde{\delta} \sim \text{Log-}\mathcal{N}(\mu_d, \sigma_d)$.

Taking as reference the RN $\mathbf{A}_0$, the actual signal strength received $P_r(\mathbf{A}_{j-1}, \mathbf{A}_j)$ between two neighboring nodes $\mathbf{A}_{j-1}$ and $\mathbf{A}_j$ for every j without shadowing effects is computed by

$$P_r(\mathbf{A}_{j-1}, \mathbf{A}_j)_{dB} = (P_T)_{dB} - 10\eta\log\left[d(\mathbf{A}_{j-1}, \mathbf{A}_j)\right] \quad (16)$$

The received signal strength $\tilde{P}_r(\mathbf{A}_{j-1}, \mathbf{A}_j)_{dB}$ with shadowing effects is computed by $\tilde{P}_r(\mathbf{A}_{j-1}, \mathbf{A}_j)_{dB} = P_r(\mathbf{A}_{j-1}, \mathbf{A}_j)_{dB} - \chi_{\sigma_{\mathbf{A}_{j-1},\mathbf{A}_j}}$ where $\sigma_{\mathbf{A}_{j-1},\mathbf{A}_j}$ is the gaussian noise standard deviation, which is proportional to the actual received signal strength $P_r(\mathbf{A}_{j-1}, \mathbf{A}_j)_{dB}$. Hence, the hop length with a measurement error is calculated by

$$D(\mathbf{A}_{j-1}, \mathbf{A}_j) = 10^{\frac{(P_T)_{dB} - \tilde{P}_r(\mathbf{A}_{j-1},\mathbf{A}_j)_{dB}}{10\eta}} \quad (17)$$

Replacing $\tilde{P}_r(\mathbf{A}_{j-1}, \mathbf{A}_j)_{dB} = P_r(\mathbf{A}_{j-1}, \mathbf{A}_j)_{dB} - \chi_{\sigma_{\mathbf{A}_{j-1},\mathbf{A}_j}}$ in equation (17), the single hop length is given by

$$D(\mathbf{A}_{j-1}, \mathbf{A}_j) = e^{\ln(d(\mathbf{A}_{j-1},\mathbf{A}_j)) + \frac{\left(\chi_{\sigma_{\mathbf{A}_{j-1},\mathbf{A}_j}}\right)\ln(10)}{10\eta}} \quad (18)$$

for $j = 1, 2, 3, \ldots, n_A - 1$. Therefore, the estimated separation distance δ_A formed in the path from the RN $\mathbf{A}_0$ to the NOI $\mathbf{Z}$ is obtained by

$$\delta_A = \sum_{j=1}^{n_A-1} D(\mathbf{A}_{j-1}, \mathbf{A}_j) + D(\mathbf{A}_{n_A-1}, \mathbf{Z}) \quad (19)$$

where $D(\mathbf{A}_{n_A-1}, \mathbf{Z}) = e^{\ln(d(\mathbf{A}_{n_A-1},\mathbf{Z})) + \frac{\left(\chi_{\sigma_{\mathbf{A}_{n_A-1},\mathbf{Z}}}\right)\ln(10)}{10\eta}}$ is an approximation of the real distance $d(\mathbf{A}_{n_A-1}, \mathbf{Z})$ of the neighboring node $\mathbf{A}_{n_A-1}$ to the NOI $\mathbf{Z}$. Therefore, the estimated separation range δ_A formed in the path from the RN $\mathbf{A}_0$ to the NOI $\mathbf{Z}$ is computed by

$$\delta_A = \sum_{j=1}^{n_A-1} e^{\ln(d(\mathbf{A}_{j-1},\mathbf{A}_j)) + \frac{\left(\chi_{\sigma_{\mathbf{A}_{j-1},\mathbf{A}_j}}\right)\ln(10)}{10\eta}} + e^{\ln(d(\mathbf{A}_{n_A-1},\mathbf{Z})) + \frac{\left(\chi_{\sigma_{\mathbf{A}_{n_A-1},\mathbf{Z}}}\right)\ln(10)}{10\eta}} \quad (20)$$

$$\delta_A = \sum_{j=1}^{n_A-1} d(\mathbf{A}_{j-1}, \mathbf{A}_j)\, 10^{\frac{\chi_{\sigma_{\mathbf{A}_{j-1},\mathbf{A}_j}}}{10\eta}} + d(\mathbf{A}_{n_A-1}, \mathbf{Z})\, 10^{\frac{\chi_{\sigma_{\mathbf{A}_{n_A-1},\mathbf{Z}}}}{10\eta}} \quad (21)$$

Assuming that the NOI $\mathbf{Z}$ is moving, the range δ_A from the RN $\mathbf{A}_0$ to the NOI $\mathbf{Z}$ will be affected by a beta random variable φ_A due to the mobility of the NOI $\mathbf{Z}$. Therefore, the range δ_A from the RN $\mathbf{A}_0$ to the NOI $\mathbf{Z}$ is computed through

$$\delta_A = \sum_{j=1}^{n_A-1} d(\mathbf{A}_{j-1}, \mathbf{A}_j)\, 10^{\frac{\chi_{\sigma_{\mathbf{A}_{j-1},\mathbf{A}_j}}}{10\eta}} + d(\mathbf{A}_{n_A-1}, \mathbf{Z})\, 10^{\frac{\chi_{\sigma_{\mathbf{A}_{n_A-1},\mathbf{Z}}}}{10\eta}} + \varphi_A \quad (22)$$

where the beta random variable φ_A is weighted by the factor λ_A proportional to the real separation distance between the NOI $\mathbf{Z}$ and the RN $\mathbf{A}_0$, i.e., $0 < \varphi_A < 1/\lambda_A$. Now, we assume in equation (22) that the Gaussian and beta random variables are independent. We observe in (22) that the parameter δ_A is the estimated range between the RN $\mathbf{A}_0$ and the NOI $\mathbf{Z}$ obtained in the instant of time $\tau = t$. Asumming that the localization of a single node is not dependent on others instant of time, namely, $\tau = 1, 2, 3, \ldots, t$, then, by using the equation (22) we can estimate the position of the NOI $\mathbf{Z}$ regardless of the value of the instant of time τ.

IV. LOCALIZATION ALGORITHMS ANALYZED

A. MULTILATERATION ALGORITHM (MA)

By taking Figure 4 as our reference, we can obtain the position of the NOI $\mathbf{Z}$ using the trilateration localization algorithm of the RNs $\mathbf{A}_0$, $\mathbf{B}_0$ and $\mathbf{C}_0$. However, for 4 or more RNs, we use the Multilateration localization algorithm to estimate the position of the NOI $\mathbf{Z}$ with coordinates (x, y) in [39]. In a node network with $\mathcal{N}$ number of RNs, the estimated distance δ_i between the mobile NOI $\mathbf{Z}$ and the RN i, is calculated

through the Pythagorean theorem as follows

$$\delta_i^2 = (x_i - \tilde{x})^2 + (y_i - \tilde{y})^2, \quad i = 1, 2, \ldots, N. \tag{23}$$

where $(\tilde{x}, \tilde{y})$ is the estimated position of the NOI $\mathbf{Z}$. Equation (23) implies a non-linear problem. By solving the subtraction $\delta_i^2 - \delta_1^2$, the non-linear problem becomes a linear problem, which can be solved by a Least Squares (LS) estimator; and we finally get

$$2\tilde{x}x_i + 2\tilde{y}y_i - 2\tilde{x}x_1 - 2\tilde{y}y_1 = x_i^2 + y_i^2 - x_1^2 - y_1^2 - \delta_i^2 + \delta_1^2. \tag{24}$$

Expanding the equation (24) for $i = 2, 3, \ldots, N$, and redefining it in a matrix form [39] we get

$$\begin{bmatrix} x_2 - x_1 & y_2 - y_1 \\ \vdots & \vdots \\ x_N - x_1 & y_N - y_1 \end{bmatrix} \begin{bmatrix} \tilde{x} \\ \tilde{y} \end{bmatrix} = \frac{1}{2} \begin{bmatrix} x_2^2 + y_2^2 - x_1^2 - y_1^2 - \delta_2^2 + \delta_1^2 \\ \vdots \\ x_N^2 + y_N^2 - x_1^2 - y_1^2 - \delta_N^2 + \delta_1^2 \end{bmatrix}. \tag{25}$$

Then, the linear problem can be formulated as

$$\mathbf{H}\tilde{\mathbf{p}} = \mathbf{b}. \tag{26}$$

where $\mathbf{H} = \begin{bmatrix} x_2 - x_1 & y_2 - y_1 \\ \vdots & \vdots \\ x_N - x_1 & y_N - y_1 \end{bmatrix}$, $\tilde{\mathbf{p}} = \begin{bmatrix} \tilde{x} \\ \tilde{y} \end{bmatrix}$ and $\mathbf{b}$ is a random vector given by

$$\mathbf{b} = \frac{1}{2} \begin{bmatrix} x_2^2 + y_2^2 - x_1^2 - y_1^2 - \delta_2^2 + \delta_1^2 \\ \vdots \\ x_N^2 + y_N^2 - x_1^2 - y_1^2 - \delta_N^2 + \delta_1^2 \end{bmatrix}. \tag{27}$$

Finally, the estimated position $\tilde{\mathbf{p}}$ of the NOI $\mathbf{Z}$ is computed by next equation

$$\tilde{\mathbf{p}} = (\mathbf{H}^T\mathbf{H})^{-1}\mathbf{H}^T\mathbf{b}. \tag{28}$$

Therefore, through equation (28) we get that the position $\tilde{\mathbf{p}}$ of the NOI $\mathbf{Z}$ is computed by a Least Squares estimator (LS).

B. WEIGHTED MULTILATERATION ALGORITHM (WMA)

There is a variety of range-based localization techniques that estimate the position of a NOI. Some of those techniques are the hyperbolic positioning algorithm (Multilateration) [21], weighted hyperbolic positioning algorithm (Weighted Multilateration) [21], circular positioning algorithm [21], MDS algorithm [40], etc. The hyperbolic and weighted hyperbolic positioning algorithms solve the localization problem through Multilateration [21], [39], where a resulting linear equation is easily solved by using a least squares estimator. The circular and weighted circular positioning algorithms computes iteratively the position of the NOI using the gradient descent method [45], iteratively until convergence is reached. The MDS algorithm computes the position of the NOI using a spectral decomposition of a matrix of the separation ranges between the RNs and the NOI. However, this method implies a computationally high cost, since, it is a centralized algorithm, reason why a single node requires a higher number of computing operations in order to estimate the position of the NOI [40]. Therefore, we opt for the weighted Multilateration algorithm, since this method is an improvement of the classic Multilateration algorithm; the WMA algorithm only adds a covariance matrix into the MA algorithm; hence, the MA and WMA algorithms have the same computational complexity order. The covariance matrix contains the information of the estimated distance between the NOI and the respective RNs, so the covariance matrix includes the weights on how accurate the estimated distances are between the NOI and the RNs closest to their real values, which implies a higher accuracy in the localization of the NOI.

Taking Figure 4 as a reference, the distance δ_A from the RN $\mathbf{A}_0$ to NOI $\mathbf{Z}$ can be estimated using equation (22). However, in a network with N number of RNs, we get the estimated distance δ_i between the mobile node and the RN i given by $\delta_i = X_i + \varphi_i$, where $X_i \sim \text{Log-}\mathcal{N}(\mu_{d_i}, \sigma_{d_i})$ due to the environmental features. The position of the mobile node can be estimated using the Weighted Multilateration Algorithm as follows

$$\tilde{\mathbf{p}} = \left(\mathbf{H}^T\mathbf{S}^{-1}\mathbf{H}\right)^{-1}\mathbf{H}^T\mathbf{S}^{-1}\mathbf{b} \tag{29}$$

where $\mathbf{S}$ is the covariance matrix of the random vector $\mathbf{b}$ given by

$$\mathbf{S} = \begin{bmatrix} \text{Var}\left(\delta_1^2\right) + \text{Var}(\delta_2^2) & \text{Var}\left(\delta_1^2\right) & \cdots & \text{Var}\left(\delta_1^2\right) \\ \text{Var}\left(\delta_1^2\right) & \text{Var}\left(\delta_1^2\right) + \text{Var}(\delta_3^2) & \cdots & \text{Var}\left(\delta_1^2\right) \\ \vdots & \vdots & \ddots & \vdots \\ \text{Var}\left(\delta_1^2\right) & \text{Var}\left(\delta_1^2\right) & \cdots & \text{Var}\left(\delta_1^2\right) + \text{Var}(\delta_N^2) \end{bmatrix} \tag{30}$$

From equation (30), we get that the elements of the covariance matrix $\mathbf{S}$ depend on the real separation distance from the RN i to NOI. By definition the variance of a random variable as $\text{Var}(\psi) = \text{E}\left(\psi^2\right) - [\text{E}(\psi)]^2$, where E is the mean or expected value; then, we can get the variance of the random variable δ_i^2 as follows

$$\text{Var}\left(\delta_i^2\right) = \text{E}\left(\delta_i^4\right) - \left[\text{E}\left(\delta_i^2\right)\right]^2 \tag{31}$$

where

$$\delta_i^2 = (X_i + \varphi_i)^2 = X_i^2 + 2X_i\varphi_i + \varphi_i^2$$

$$\delta_i^4 = (X_i + \varphi_i)^4 = X_i^4 + 4X_i^3\varphi_i + 6X_i^2\varphi_i^2 + 4X_i\varphi_i^3 + \varphi_i^4$$

$$\text{E}\left(\delta_i^4\right) = \text{E}\left(X_i^4\right) + 4\text{E}\left(X_i^3\right)\text{E}(\varphi_i) + 6\text{E}\left(X_i^2\right)\text{E}\left(\varphi_i^2\right) + 4\text{E}(X_i)\,\text{E}\left(\varphi_i^3\right) + \text{E}\left(\varphi_i^4\right)$$

$$\left[\mathrm{E}\left(\delta_i^2\right)\right]^2 = \left[\mathrm{E}\left(X_i^2\right) + 2\mathrm{E}\left(X_i\right)\mathrm{E}\left(\varphi_i\right) + \mathrm{E}\left(\varphi_i^2\right)\right]^2$$
$$= \mathrm{E}^2\left(X_i^2\right) + 4\mathrm{E}\left(\varphi_i\right)\mathrm{E}(X_i)\mathrm{E}(X_i^2) + 4\mathrm{E}^2\left(X_i\right)\mathrm{E}^2\left(\varphi_i\right)$$
$$+ 2\mathrm{E}(\varphi_i^2)\mathrm{E}(X_i^2) + 4\mathrm{E}\left(X_i\right)\mathrm{E}(\varphi_i)\mathrm{E}(\varphi_i^2) + \mathrm{E}^2\left(\varphi_i^2\right)$$

Finally, the parameter $\mathrm{Var}\left(\delta_i^2\right)$ is obtained by

$$\mathrm{Var}\left(\delta_i^2\right) = \mathrm{Var}\left(X_i^2\right) + \mathrm{Var}\left(\varphi_i^2\right) + 4\mathrm{Var}\left(\varphi_i X_i\right) + 4\mathrm{E}\left(X_i^3\right)\mathrm{E}\left(\varphi_i\right) + 4\mathrm{E}\left(X_i\right)\mathrm{E}\left(\varphi_i^3\right) - 4\mathrm{E}\left(\varphi_i\right)\mathrm{E}\left(X_i\right)\mathrm{E}\left(X_i^2\right) - 4\mathrm{E}\left(X_i\right)\mathrm{E}\left(\varphi_i\right)\mathrm{E}\left(\varphi_i^2\right) \quad (32)$$

Equation (32) shows that the variance of the estimated distance δ_i between an RN i and the NOI depend on the statistical parameters of the random variables X_i and φ_i with log-normal distribution and beta distribution, respectively. Therefore, the term $\mathrm{Var}\left(\delta_i^2\right)$ depends on the real distance between the RN i and the NOI; however, in an actual implementation it is necessary to approximate the estimated distance δ_i to its real value for each RN i.

C. PROBABILISTIC MULTILATERATION ALGORITHM (PMA)

This approach estimates the position of the NOI using the position of the RNs and the ranges between the NOI and the RNs. The main goal of this approach is to reduce the flaws such as uncertainty, non-consistency and ambiguity that affect the Multilateration algorithm [46]. Assuming that for every RN i we define a pdf $P_i(x, y)$ that assigns the probability of finding a node in the plane (or space), then, for 3 or more RNs we define a joint probability $P_B(x, y)$, where B is the set of N RNs. Due to the independence of the separation ranges between the NOI and the RNs, the pdfs of the RNs are independent of each other. Therefore, the joint pdf $P_B(x, y)$ can be calculated as a product of independent pdfs, as shown below

$$P_B(x, y) = \prod_{i=1}^{N} P_i(x, y) \quad (33)$$

Equation (33) indicates that the position (x, y) of the NOI will be where the joint pdf $P_B(x, y)$ reaches its maximum value. In the case of range-free algorithms the pdf is unknown; therefore, we use a gaussian generic pdf whose parameters depend on the position of the NOI and the separation distance between the RNs and the NOI. Assuming, that for each RN i the pdf $P_i(x, y)$ is Gaussian with parameters (μ_i, σ_i). Therefore, the joint pdf $P_B(x, y)$ is expressed by

$$P_B(x, y) = \prod_{i=1}^{N} \frac{1}{\mathcal{N}_i} e^{-\frac{1}{2}\left[\frac{\sqrt{(x-x_i)^2+(y-y_i)^2}-\mu_i}{\sigma_i}\right]^2} \quad (34)$$

where $\mathcal{N}_i$ is a normalization factor whose product is unitary, i.e., $\prod_{i=1}^{N} 1/\mathcal{N}_i = 1$, μ_i is the observed separation distance between an RN i and the NOI, which is affected by unwanted noise, and σ_i is the standard deviation of unwanted noise, which is proportional to the separation distance between a RN i and the NOI. In order to find the maximum value of $P_B(x, y)$, we calculate the partial derivates in Equation (34) with respect to the coordinates (x, y) of the position of the NOI and we get the following equations

$$\frac{\partial P_B(x, y)}{\partial x} = \sum_{i=1}^{N} \frac{\left(\sqrt{(x-x_i)^2+(y-y_i)^2}-\mu_i\right)(x-x_i)}{\sigma_i\sqrt{(x-x_i)^2+(y-y_i)^2}} = 0 \quad (35)$$

$$\frac{\partial P_B(x, y)}{\partial y} = \sum_{i=1}^{N} \frac{\left(\sqrt{(x-x_i)^2+(y-y_i)^2}-\mu_i\right)(y-y_i)}{\sigma_i\sqrt{(x-x_i)^2+(y-y_i)^2}} = 0 \quad (36)$$

$$\left[\sum_{i=1}^{N} \frac{\left(\sqrt{(x-x_i)^2+(y-y_i)^2}-\mu_i\right)(x-x_i)}{\sigma_i\sqrt{(x-x_i)^2+(y-y_i)^2}}\right]^2 + \left[\sum_{i=1}^{N} \frac{\left(\sqrt{(x-x_i)^2+(y-y_i)^2}-\mu_i\right)(y-y_i)}{\sigma_i\sqrt{(x-x_i)^2+(y-y_i)^2}}\right]^2 = 0 \quad (37)$$

Equation (37) is obtained from the sum of the cuadratic terms in equations (35)-(36), so it is a non-linear problem with two unknown variables. The non-linear problem is solved by applying the Newton Raphson algorithm, where the starting point is the centroid of the positions of the RNs.

V. IMPROVED PROBABILISTIC MULTILATERATION APPROACH

This approach computes the position of a NOI assuming the position of the RNs and the ranges between them and the NOI in presence of unwanted noise. We assume that the separation distance between an RN i and the NOI is given by $z_i = \sqrt{(x-x_i)^2+(y-y_i)^2}, i = 1, 2, \ldots, N$; μ_i is the observed distance with Additive Gaussian White Noise (AGWN) between the RN i and the NOI, and σ_i is the standard deviation of gaussian noise, which is proportional to the separation distance between the RN i and the NOI. Equation (34) can be expressed as

$$P_B(x, y) = \left[\prod_{i=1}^{N} \frac{1}{\mathcal{N}_i}\right] \exp\left(\frac{-1}{2\sigma_i^2}\sum_{i=1}^{N}(z_i-\mu_i)^2\right) \quad (38)$$

We assume a set of actual distances z_i in a vectorial form as $\mathbf{z} = [z_1, z_2, \ldots, z_N]^T$ and a set of observed distances μ_i

in a vectorial form as $\mathbf{u} = [\mu_1, \mu_2, \ldots, \mu_N]^T$; the position of the NOI is assumed as the vector $\mathbf{x} = [x, y]^T$. Therefore, from Equation (38) we get the cost function $F(\mathbf{x})$ given by

$$F(\mathbf{x}) = \frac{1}{\sigma_i^2} \sum_{i=1}^{N} (z_i - \mu_i)^2 = \mathbf{e}^T \mathbf{K}^{-1} \mathbf{e} \tag{39}$$

where $\mathbf{e} = \mathbf{z} - \mathbf{u}$ is a vector with the residues between the real distances and the estimated distances between the NOI and the RNs. We observe that the cost function $F(\mathbf{x})$ involves a non-linear problem. The solution for this type of problems requires higher computational cost and it further implies convergence in local minimum. In order to solve this problem, we introduce an iterative algorithm based on an LS estimator where the Taylor series of first order is used to get an approximation of the position of the NOI. Therefore, the vector $\mathbf{z}$ is used as a function vector, which can be expressed by the Taylor series of first order, i.e., $\mathbf{z} = \mathbf{z}_0 + \mathcal{J}[\mathbf{x} - \mathbf{x}_0]$, where $\mathbf{x}_0$ is the starting point and $\mathcal{J}$ is the Jacobian matrix of dimension Nx2 given by

$$\begin{aligned}\mathcal{J} &= \begin{bmatrix} \frac{\partial z_1}{\partial \mathrm{x}} & \frac{\partial z_1}{\partial \mathrm{y}} \\ \frac{\partial z_2}{\partial \mathrm{x}} & \frac{\partial z_2}{\partial \mathrm{y}} \\ \vdots & \vdots \\ \frac{\partial z_N}{\partial \mathrm{x}} & \frac{\partial z_N}{\partial \mathrm{y}} \end{bmatrix} \\ &= \begin{bmatrix} \frac{x-x_1}{\sqrt{(x-x_1)^2+(y-y_1)^2}} & \frac{y-y_1}{\sqrt{(x-x_1)^2+(y-y_1)^2}} \\ \frac{x-x_2}{\sqrt{(x-x_2)^2+(y-y_2)^2}} & \frac{y-y_2}{\sqrt{(x-x_2)^2+(y-y_2)^2}} \\ \vdots & \vdots \\ \frac{x-x_N}{\sqrt{(x-x_N)^2+(y-y_N)^2}} & \frac{y-y_N}{\sqrt{(x-x_N)^2+(y-y_N)^2}} \end{bmatrix} \end{aligned} \tag{40}$$

By replacing $\mathbf{z} = \mathbf{z}_0 + \mathcal{J}[\mathbf{x} - \mathbf{x}_0]$ in Equation (39) we get

$$\begin{aligned} F(\mathbf{x}) = {} & [\mathbf{z}_0 + \mathcal{J}\mathbf{x} - \mathcal{J}\mathbf{x}_0 - \mathbf{u}]^T \mathbf{K}^{-1} \\ & [\mathbf{z}_0 + \mathcal{J}\mathbf{x} - \mathcal{J}\mathbf{x}_0 - \mathbf{u}] \end{aligned} \tag{41}$$

By expanding Equation (41) we get

$$\begin{aligned} F(\mathbf{x}) = {} & \mathbf{z}_0^T \mathbf{K}^{-1} \mathbf{z}_0 + \mathbf{z}_0^T \mathbf{K}^{-1} \mathcal{J}\mathbf{x} - \mathbf{z}_0^T \mathbf{K}^{-1} \mathcal{J}\mathbf{x}_0 - \mathbf{z}_0^T \mathbf{K}^{-1} \mathbf{u} \\ & + \mathbf{x}^T \mathcal{J}^T \mathbf{K}^{-1} \mathbf{z}_0 + \mathbf{x}^T \mathcal{J}^T \mathbf{K}^{-1} \mathcal{J}\mathbf{x} - \mathbf{x}^T \mathcal{J}^T \mathbf{K}^{-1} \mathcal{J}\mathbf{x}_0 \\ & - \mathbf{x}^T \mathcal{J}^T \mathbf{K}^{-1} \mathbf{u} - \mathbf{x}_0^T \mathcal{J}^T \mathbf{K}^{-1} \mathbf{z}_0 - \mathbf{x}_0^T \mathcal{J}^T \mathbf{K}^{-1} \mathcal{J}\mathbf{x} \\ & + \mathbf{x}_0^T \mathcal{J}^T \mathbf{K}^{-1} \mathcal{J}\mathbf{x}_0 + \mathbf{x}_0^T \mathcal{J}^T \mathbf{K}^{-1} \mathbf{u} - \mathbf{u}^T \mathbf{K}^{-1} \mathbf{z}_0 \\ & - \mathbf{u}^T \mathbf{K}^{-1} \mathcal{J}\mathbf{x} + \mathbf{u}^T \mathbf{K}^{-1} \mathcal{J}\mathbf{x}_0 + \mathbf{u}^T \mathbf{K}^{-1} \mathbf{u} \end{aligned} \tag{42}$$

Deriving the cost function $F(\mathbf{x})$ in Equation (42) with respect to the position $\mathbf{x}$ of the NOI, we get the following equation

$$\begin{aligned} \frac{\partial F(\mathbf{x})}{\partial \mathbf{x}} = 2 \Big[& \mathcal{J}^T \mathbf{K}^{-1} \mathbf{z}_0 + \mathcal{J}^T \mathbf{K}^{-1} \mathcal{J}\mathbf{x} - \mathcal{J}^T \mathbf{K}^{-1} \mathcal{J}\mathbf{x}_0 \\ & - \mathcal{J}^T \mathbf{K}^{-1} \mathbf{u} \Big] = 0 \end{aligned} \tag{43}$$

Leading the position $\mathbf{x}$ of the NOI in Equation (43), we get

$$\mathcal{J}^T \mathbf{K}^{-1} \mathcal{J}\mathbf{x} = \mathcal{J}^T \mathbf{K}^{-1} \mathcal{J}\mathbf{x}_0 + \mathcal{J}^T \mathbf{K}^{-1} [\mathbf{u} - \mathbf{z}_0] \tag{44}$$

$$\mathbf{x} = \mathbf{x}_0 + \left[\mathcal{J}^T \mathbf{K}^{-1} \mathcal{J} \right]^{-1} \mathcal{J}^T \mathbf{K}^{-1} [\mathbf{u} - \mathbf{z}_0] \tag{45}$$

Equation (45) is the solution for Equation (39). We observe that equation (45) presents an optimization problem, which is recursively solved until convergence of the position $\mathbf{x}$ of the NOI is reached. Therefore, Equation (45) is recursively expressed as follows

$$\mathbf{x}^{k+1} = \mathbf{x}^k + \left[\mathcal{J}^T \mathbf{K}^{-1} \mathcal{J} \right]^{-1} \mathcal{J}^T \mathbf{K}^{-1} [\mathbf{u} - \mathbf{z}_k] \tag{46}$$

We observe in Equation (46) that for each iteration k the Jacobian matrix and the vector $\mathbf{z}$ are updated until the term $\mathbf{u} - \mathbf{z}_k$ tends to zero. We compute the centroid of the positions of the RNs as the starting point $\mathbf{x}_0$.

In Equation (46) the *damping factor* μ is added, which enhances the accuracy of the localization of the NOI. Then, the position of the NOI is recursively computed by the following equation

$$\begin{aligned} \mathbf{x}^{k+1} = {} & \mathbf{x}^k + \left[\mathcal{J}^T \mathbf{K}^{-1} \mathcal{J} + \mu \, \mathrm{diag} \left(\mathcal{J}^T \mathbf{K}^{-1} \mathcal{J} \right) \right]^{-1} \\ & \times \mathcal{J}^T \mathbf{K}^{-1} [\mathbf{u} - \mathbf{z}_k] \end{aligned} \tag{47}$$

We observe in Equation (47) that the damping factor $\mu > 0$ affects the elements of the main diagonal of the matrix $\mathcal{J}^T \mathcal{J}$. The *damping factor* μ is a factor that modifies the curvature of the cost function $F(\mathbf{x})$.

VI. RESULTS

This section shows the performance of the localization algorithms Multilateration Algorithm (MA), Weighted Multilateration Algorithm (WMA), Probabilistic Multilateration Approach (PMA) and Improved PMA. The mobility parameters of the NOI are $(\alpha, \beta) = (2.1, 3.2)$, which were obtained through the average of 100 simulations. In addition the parameters α, β of the beta distribution are estimated when obtaining the beta distribution due to the mobility of the NOI.

The aforementioned localization techniques are evaluated in MATLAB over a sensing area which is 100 m x 100 m where the nodes are randomly distributed and the RNs are evenly placed in a triangular area with fixed positions. The RNs are collinears to a circumference of radius R_{max} that defines the maximum separation distance between them. The coverage radius R_0 of the NOI in an ad-hoc network depends on the transmitting power of the node and the receiver sensitivity. This study utilizes the log-normal Shadowing propagation model in order to estimate the RSS between the NOI and the RNs; for this propagation model we use the following parameters $n = 3.2$ and $P_T = 100$mW. We assume

TABLE 1. Test cases description.

Case	Description
1	We consider a network where 3 RNs are arranged in a solid triangular geometry and more RNs are added with random positions until we get 7 RNs.
2	In this case, RNs remain fixed with geometries of regular polygons from the triangular type of geometry to the heptagonal type.
3	In this scenario, RNs are randomly distributed within the deployment area, reason why it is difficult to get a solid distribution of the RNs.

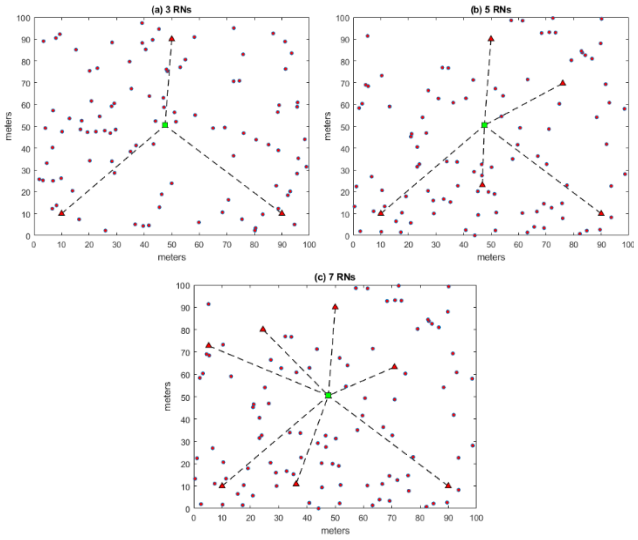

FIGURE 5. Fixed RNs with triangular geometry and randomly distributed extra nodes.

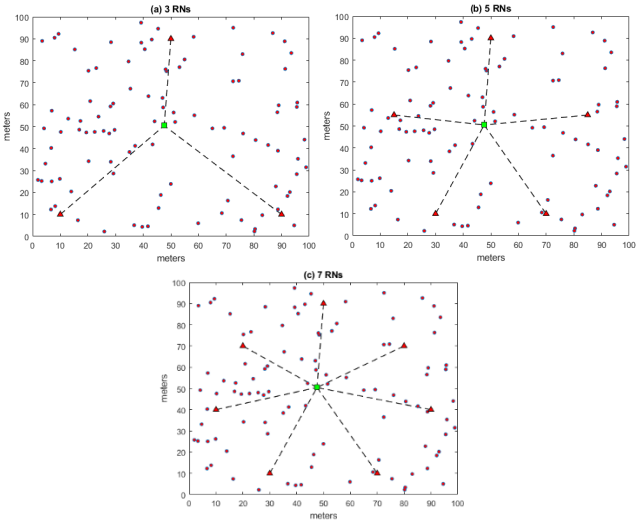

FIGURE 6. Distribution of the fixed RNs with solid geometries.

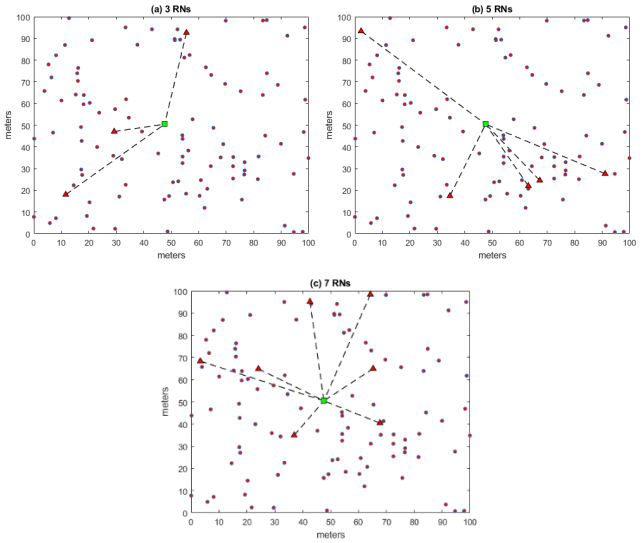

FIGURE 7. Randomly distributed RNs.

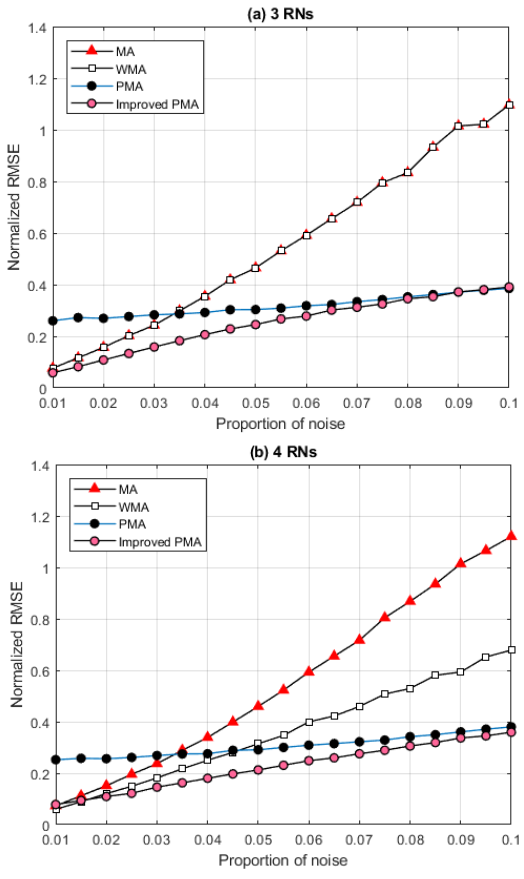

FIGURE 8. Normalized RMSE vs proportion of noise considering (a) 3 RNs and (b) 4 RNs for the first case in a single-hop network.

that a single node cannot link a connection with all nodes in the network, i.e., there is no established link, therefore the results are reported in terms of the normalized coverage radius given by R_0/R_{max}. The obtained results are shown in terms of the Normalized Root Mean Square Error (RMSE) given by $\left(\text{RMSE}/R_{max}\right)$. The reported results implied a total of 10^4 realizations to estimate the position of the NOI in each simulation scenario. The Normalized RMSE of the

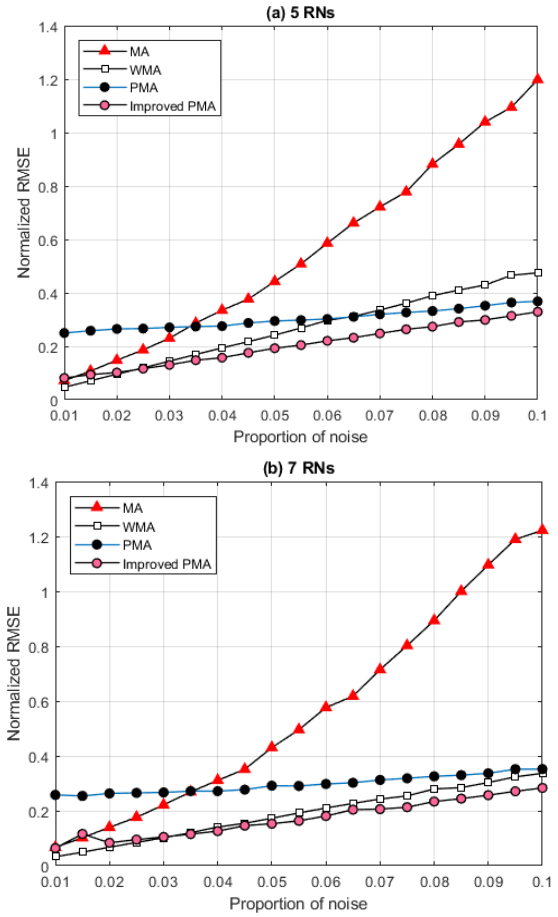

FIGURE 9. Normalized RMSE vs proportion of noise considering (a) 5 RNs and (b) 7 RNs for the first case in a single-hop network.

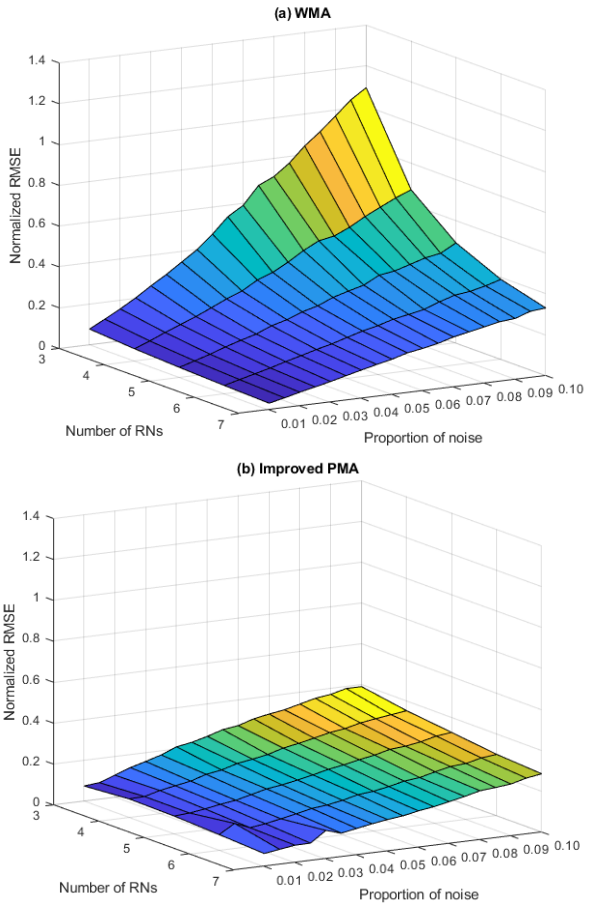

FIGURE 10. Normalized RMSE vs proportion of noise starting at 3 and up to 7 RNs for (a) WMA and (b) Improved PMA for the first case in a single-hop network.

reported localization algorithms is obtained in the instant of time $\tau = t$, which presents a single realization of the 100 realizations considered in order to estimate the mobility parameters of the NOI. Besides, we consider that there is no need to estimate the Normalized RMSE of the NOI through 100 realizations, since the positions of the NOI obtained in different instants of time $\tau = 1, 2, 3, \ldots, 100$ are independent of one another. We considered the single-hop and multi-hop scenarios to obtain the performance evaluation of the analyzed localization algorithms, where we consider the amount and geometry of the RNs. In every simulation scenario, we consider a network where the number of RNs is varied from 3 to 7 nodes and the NOI is randomly chosen within the sensing area.

A. SINGLE-HOP SCENARIO

Table 1 presents the test cases in order to evaluate the performance of the localization algorithms in terms of the Normalized RMSE.

In Figures 5, 6 and 7, we show a single example of the geometric distribution of the RNs according to the test cases described in Table 1 respectively. RNs are represented by the red triangles; the yellow square represents the NOI and the red circles are the nodes with unknown position.

The test cases were proposed in order to get different behaviors of the Normalized RMSE; for different geometric distributions such as the triangular and rectangular up to the heptagonal geometry; also increasing the number of RNs in the network starting with a triangular geometry and finally varying the number of RNs with totally random geometric distributions. The advantage of executing these test cases will indicate the ideal geometry and the necessary number of RNs N in the network to get the best performance of Normalized RMSE of the analyzed localization algorithms.

Table 2 shows the simulation parameters that determine the performance of the localization algorithms in terms of the Normalized RMSE according to the test cases of Table 1 in the single-hop and multi-hop scenarios.

1) CASE 1

Figure 8 introduces the performance of the Normalized RMSE of the analyzed localization algorithms, varying the proportion of noise. Figure 8(a) shows that the MA and WMA algorithms maintain the same performance with 3 RNs; whilst the Improved PMA algorithm has less Normalized

TABLE 2. Simulation parameters.

Parameter	Value
Networking Area	100 m x 100 m
Proportion of noise (np)	0.010, 0.015, 0.020, 0.025, …, 0.095, 0.100
Number of RNs, N	3, 4, 5, 6 y 7 nodes
Number of nodes	200 nodes
Mobility parameters	$(\alpha, \beta) = (2.1, 3.2)$
Path-loss exponent (η)	3.2
Power transmitting (P_T)	100 mW
R_{max}	89.44 m

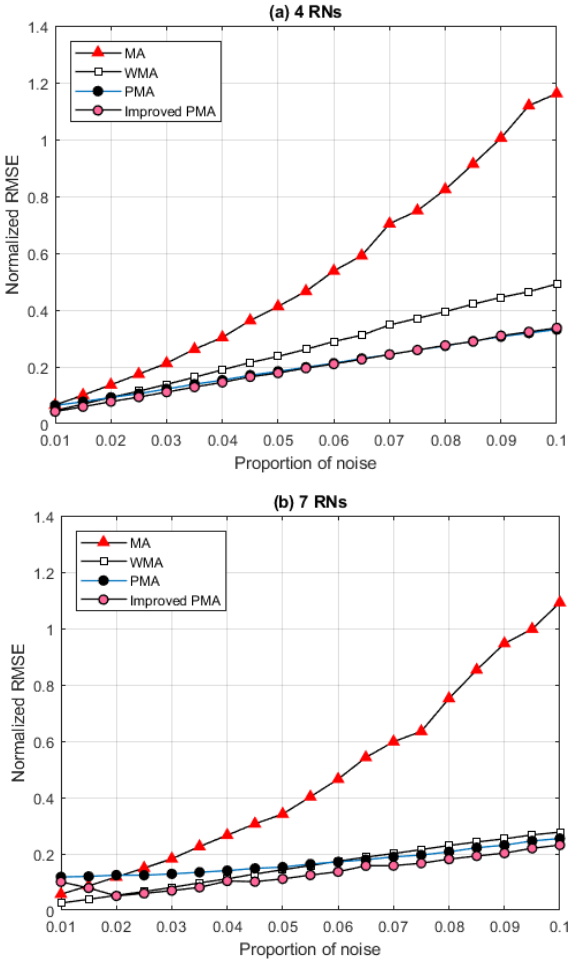

FIGURE 11. Normalized RMSE vs proportion of noise considering (a) 4 RNs and (b) 7 RNs for second case in a single hop network.

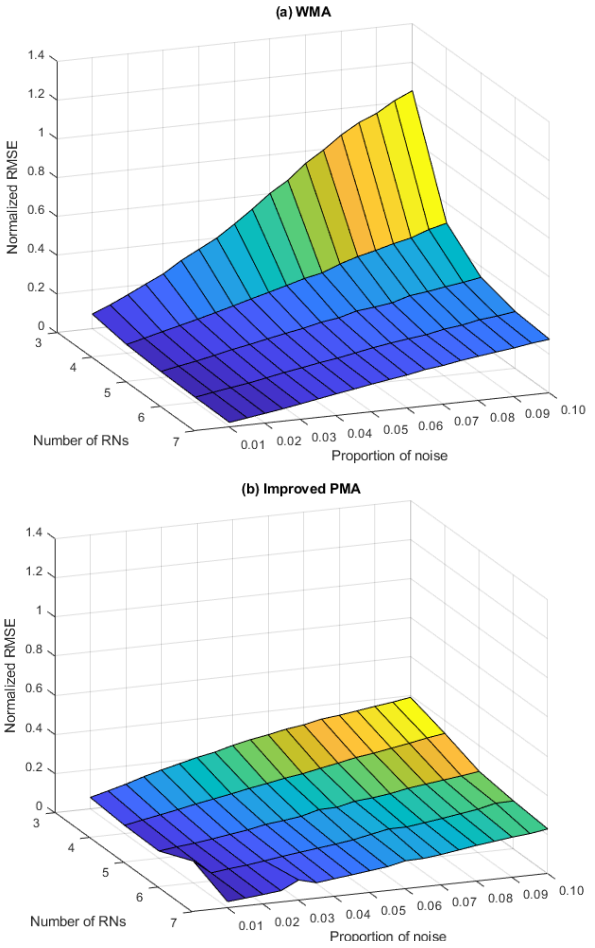

FIGURE 12. Normalized RMSE vs proportion of noise starting at 3 and up to 7 RNs for (a) WMA and (b) Improved PMA for the second case in a single-hop network.

RMSE than the MA WMA and PMA algorithms considering the variations of the noise level. However, the proposed Improved PMA approach has a rugged behavior in terms of the Normalized RMSE, since this enhancement uses an iterative algorithm until it finds the position of the NOI with the least localization error. In Figure 8(b), we can see that the Normalized RMSE decreases substantially considering 4 RNs, while the PMA algorithm displays a similar behavior in terms of Normalized RMSE for 3 and 4 RNs in the network. A similar behavior in terms of Normalized RMSE is shown in Figure 9; as the number of RNs in the network increases, the Normalized RMSE of the WMA algorithm decreases, while the PMA approach maintains its performance in terms of the Normalized RMSE increasing the number of RNs. Finally, we observe that our alternative Improved PMA reduces the Normalized RMSE as the number of RNs increases.

Assuming 7 RNs in the network, the WMA algorithm reaches less Normalized RMSE than the PMA algorithm (Figure 9(b)). However, our Improved PMA proposed algorithm performs better in terms of the Normalized RMSE than the rest of the other analyzed localization algorithms varying the noise level and the number of RNs. According to Figure 10(a), the WMA algorithm improves its performance in terms of the Normalized RMSE as the number of RNs increases. Figure 10(b) shows that the Improved PMA proposed algorithm maintains a rugged performance in terms of the Normalized RMSE as the number of RNs increases, reason why the accuracy of the localization of the NOI increases very little as the number of RNs increases. We also observe that the Improved PMA proposed algorithm presents

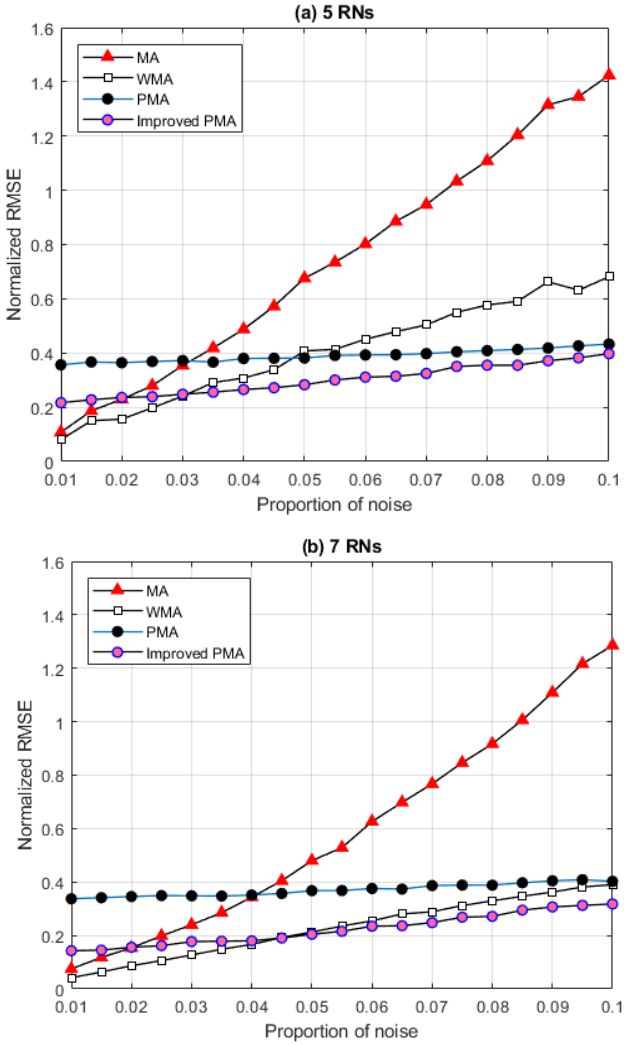

FIGURE 13. Normalized RMSE vs proportion of noise considering (a) 5 RNs and (b) 7 RNs for the third case in a single-hop network.

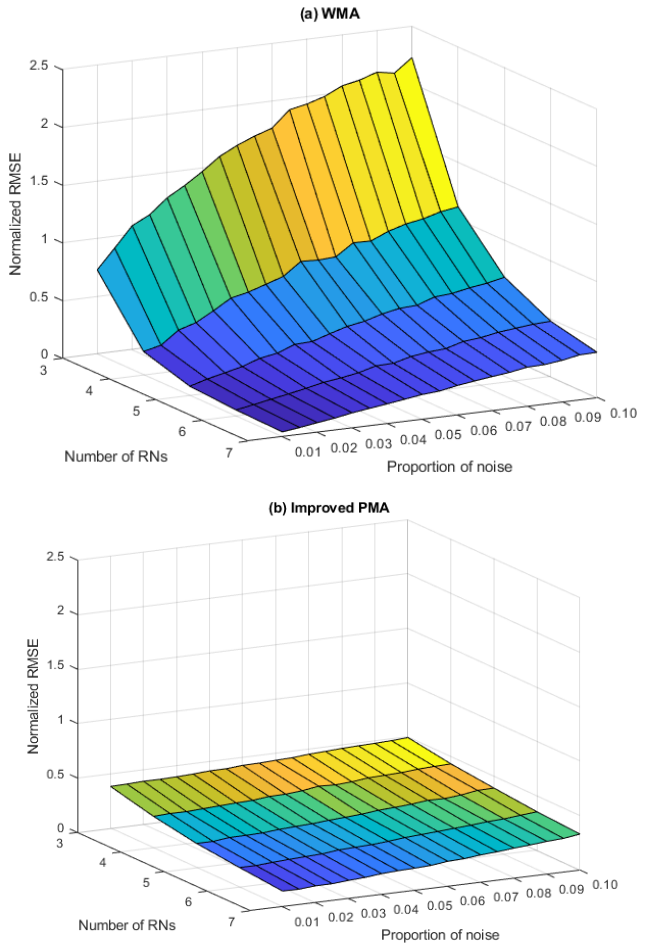

FIGURE 14. Normalized RMSE vs proportion of noise starting at 3 and up to 7 RNs for (a) WMA and (b) Improved PMA for the third case in a single-hop network.

better performance in terms of the Normalized RMSE with respect to the WMA algorithm for 3 RNs in the network.

2) CASE 2

Figure 11 presents the performance of the localization techniques regarding the normalized RMSE, considering (a) 4 RNs arranged in a solid triangular geometry and (b) 7 RNs distributed by a solid heptagonal geometry. We can see a slight diminution of the normalized RMSE considering 4 and 7 RNs arranged with solid geometries of the algorithms MA and WMA with respect to the results shown in case 1; since we get a greater coverage area of the NOI with the rectangular and heptagonal geometry than with a solid triangular geometry. However, the performance in terms of the Normalized RMSE of the MA algorithm does not show an important improvement as the number of RNs increases; since, just like in case 1, the algorithm MA presents the same normalized RMSE with 3 RNs arranged in a triangular geometry as the number of RNs increases. We can also notice that the algorithm Improved PMA displays a similar behavior in terms of the normalized RMSE as shown in Figures 8(b) and 11(a) for a network with 4 RNs, while Figure 11(b) indicates that the algorithm Improved PMA displays a little less normalized RMSE than the behavior shown in Figure 9(b) considering 7 RNs, namely, case 1. Then, the performance of the normalized RMSE of the algorithm Improved PMA does not display a significant improvement with a solid geometry distribution of the RNs. Finally, we get that the results of the normalized RMSE of the algorithms analyzed in cases 1) and 2) are very similar.

Figure 12(a) reports an improvement on the performance in regards to the normalized RMSE of the algorithm WMA augmenting the amount of RNs, where such improvement is evident starting from 4 RNs. Figure 12(b) indicates that the performance of the normalized RMSE of the proposed algorithm Improved PMA, displays a slight improvement as the amount of RNs increases, reason why the normalized RMSE of this algorithm maintains a rugged behavior as the amount of RNs increases and also the arrangement of the RNs with solid geometries does not contribute to the improvement on the performance of the normalized RMSE of the proposed algorithm PMA.

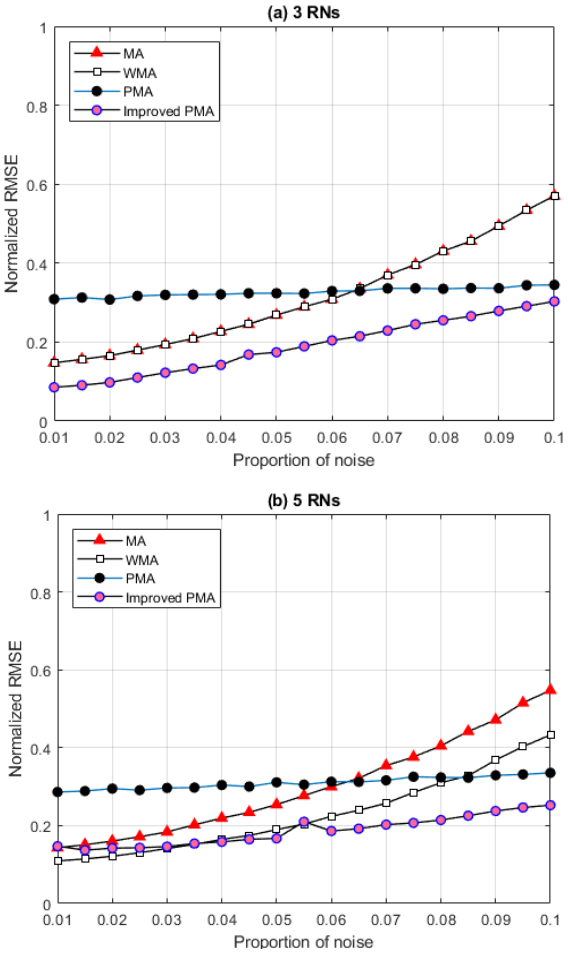

FIGURE 15. Normalized RMSE vs proportion of noise considering (a) 3 RNs and (b) 5 RNs for the first case in a multi-hop network.

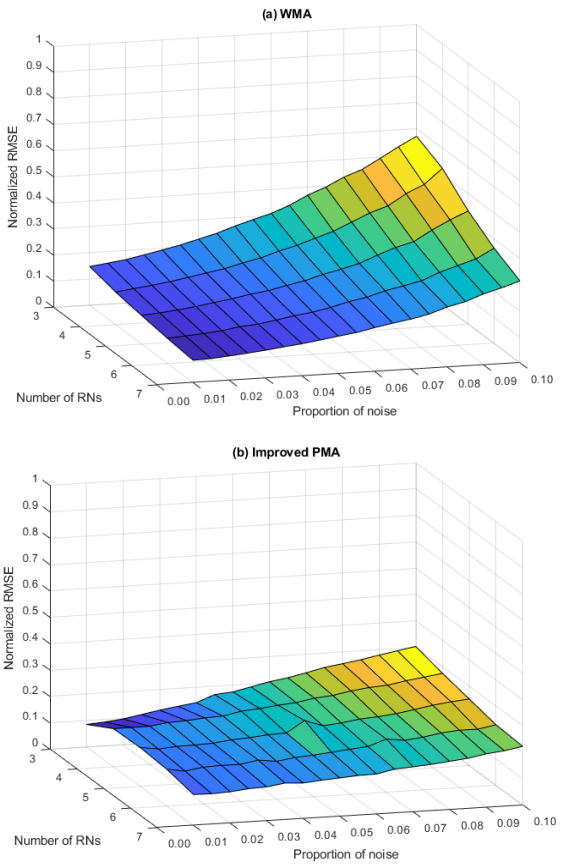

FIGURE 16. Normalized RMSE vs proportion of noise starting at 3 and up to 7 RNs for (a) WMA and (b) Improved PMA for the first case in a multi-hop network.

3) CASE 3

Figure 13(a) presents the normalized RMSE of the localization techniques considering 5 RNs randomly arranged; when comparing these results to those shown in cases 1) and 2) for 5 RNs, we get less normalized RMSE with the solid geometry than with the RNs randomly arranged. Figure 13(b) shows a diminution of the normalized RMSE of the algorithms MA and WMA by augmenting the number of RNs to 7 nodes; whereas the algorithm PMA displays the same normalized RMSE behavior for 5 and 7 RNs, therefore its performance does not improve augmenting the amount of RNs. The results shown in Figure 13 indicate that the proposed algorithm Improved PMA improves its performance in regards to the normalized RMSE as the number of RNs increases. Finally, we can see that in this case where the RNs are distributed in a random manner, the localization algorithms present a higher normalized RMSE, since there might be cases where the coverage area of the RNs is very small, therefore, we get very inaccurate localization estimations. In this case, there is no report of results on localization algorithms for 3 and 4 RNs, since the normalized RMSE of the algorithm MA for 3 and 4 RNs is very big in comparison with the other analyzed algorithms; therefore, it would not be possible to notice the performance of the algorithms WMA, PMA and Improved PMA.

Figure 14 shows the normalized RMSE of the algorithm WMA, it presents error values that are very high for 3 and 4 RNs randomly arranged. Therefore, starting at 5 RNs we get a more robust normalized RMSE value. When considering a network with 3 randomly arranged RNs, there is no guarantee of a good localization of the NOI, because the area [covered by] 3 RNs can be very small in some cases; thus, we get a lot of inaccuracy on the NOI localization. However, the algorithm improved PMA shows a rugged behavior on the normalized RMSE starting at 4 RNs, and maintains such tendency when augmenting the number of RNs.

B. MULTI-HOP SCENARIO

1) CASE 1

Figure 15 reports that the normalized RMSE of the aforementioned localization algorithms varying the proportion noise in a multi-hop scenario for (a) RNs and (b) 5 RNs. Figure 15(a) indicates that the algorithm PMA displays a steady normalized RMSE performance considering 3 RNs, because this algorithm solves the localization problem through an iterative process until it finds the position of the NOI that minimizes

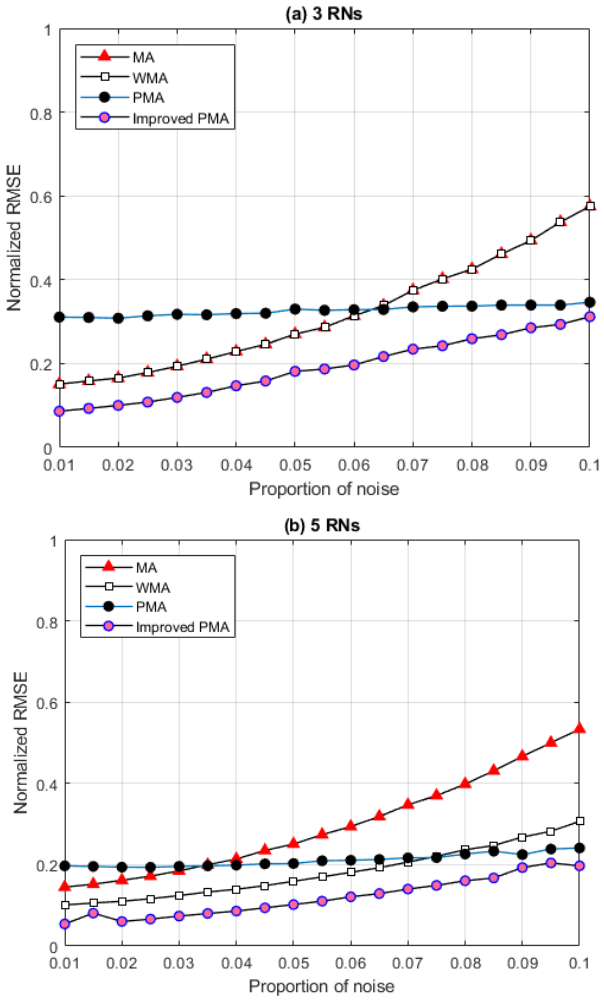

FIGURE 17. Normalized RMSE vs proportion of noise considering (a) 3 RNs and (b) 5 RNs for second case in a multi-hop network.

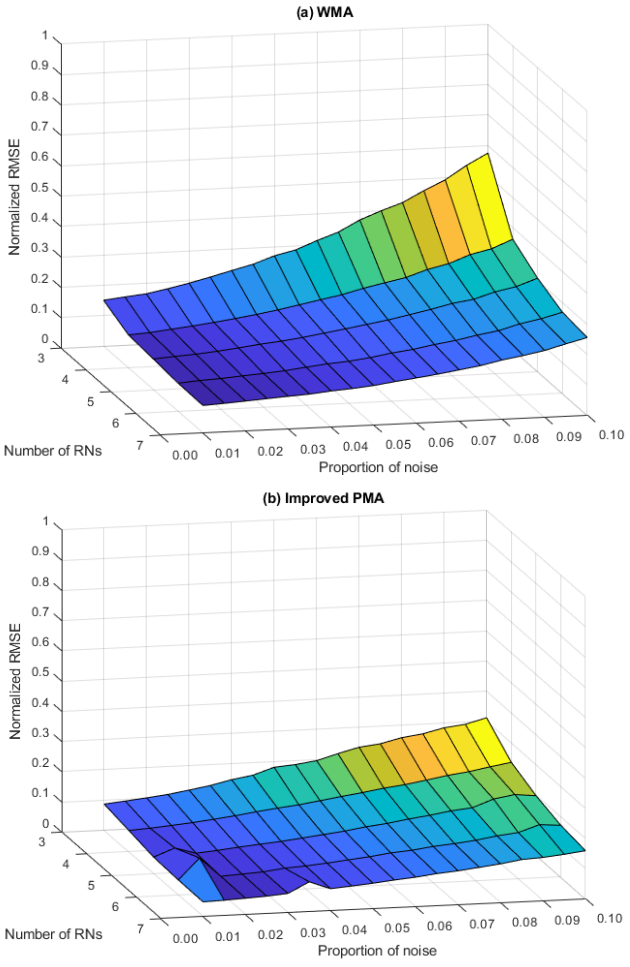

FIGURE 18. Normalized RMSE vs proportion of noise starting at 3 and up to 7 RNs for (a) WMA and (b) Improved PMA for the second case in a multi-hop network.

the cost function. For a network with 5 RNs, the algorithm PMA displays a similar performance in regards to the normalized RMSE than with 3 RNs (Figure 15(b)). However, the proposed algorithm Improved PMA displays a better performance in terms of the normalized RMSE for this case.

We can see in Figure 16(a) that there is a performance improvement in regards to the normalized RMSE of the algorithm WMA by augmenting the number of RNs. Figure 16(b) shows an even behavior of the normalized RMSE varying the proportion noise and augmenting the amount of RNs of the proposed algorithm Improved PMA. Hence, the proposed algorithm Improved PMA displays a higher sturdiness than the algorithm WMA.

2) CASE 2

Figure 17 shows the normalized RMSE of the aforementioned localization algorithms considering (a) 3 fixed RNs arranged in a solid triangular geometry and (b) 5 fixed RNs arranged in a pentagonal geometry. Considering the case of the network with 5 RNs; we can see that there is an improvement on the performance of the normalized RMSE of the localization algorithms analyzed in regards to those shown in Figure 17(a). As in case 1), the proposed algorithm Improved PMA displays less normalized RMSE than the other analyzed algorithms.

Figure 18(a) shows a significant improvement in the performance regarding the normalized RMSE of the algorithm WMA augmenting the amount of RNs using solid geometries of regular polygons. The results displayed in figure 18(b) show that the algorithm Improved PMA maintains a rugged performance in regards to the normalized RMSE; thus, there is not much variation on the normalized RMSE considering 3 or more RNs.

3) CASE 3

Figure 19(a) shows the normalized RMSE of the localization techniques considering 5 RNs randomly arranged; when comparing these results to those shown in Figure 17(b) for 5 RNs arranged with a solid pentagonal geometry, we get less normalized RMSE than with those randomly arranged.

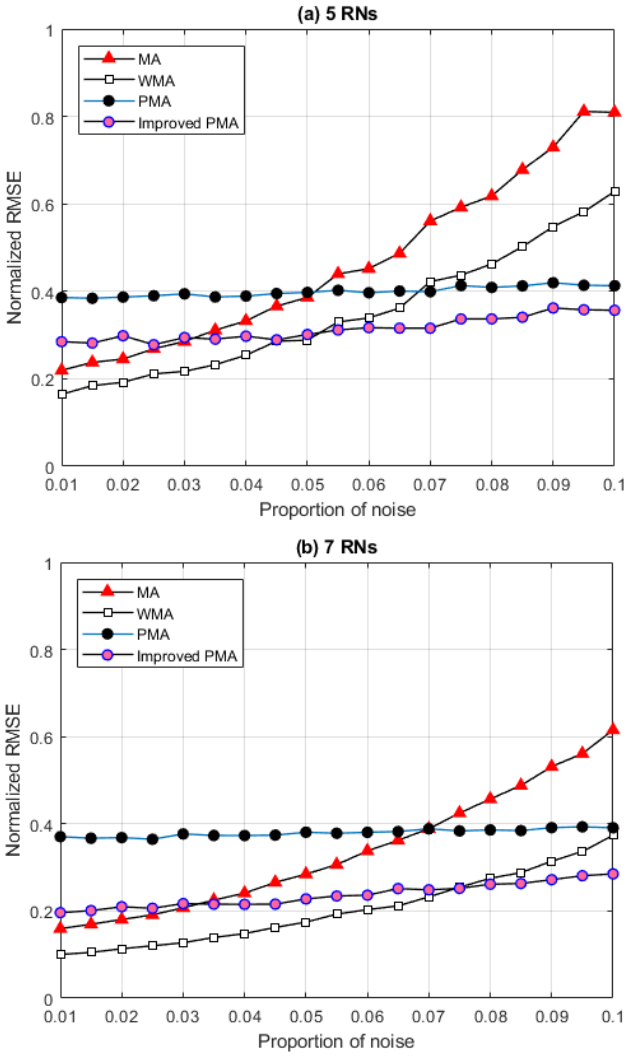

FIGURE 19. Normalized RMSE vs proportion of noise considering (a) 5 RNs and (b) 7 RNs for third case in a multi-hop network.

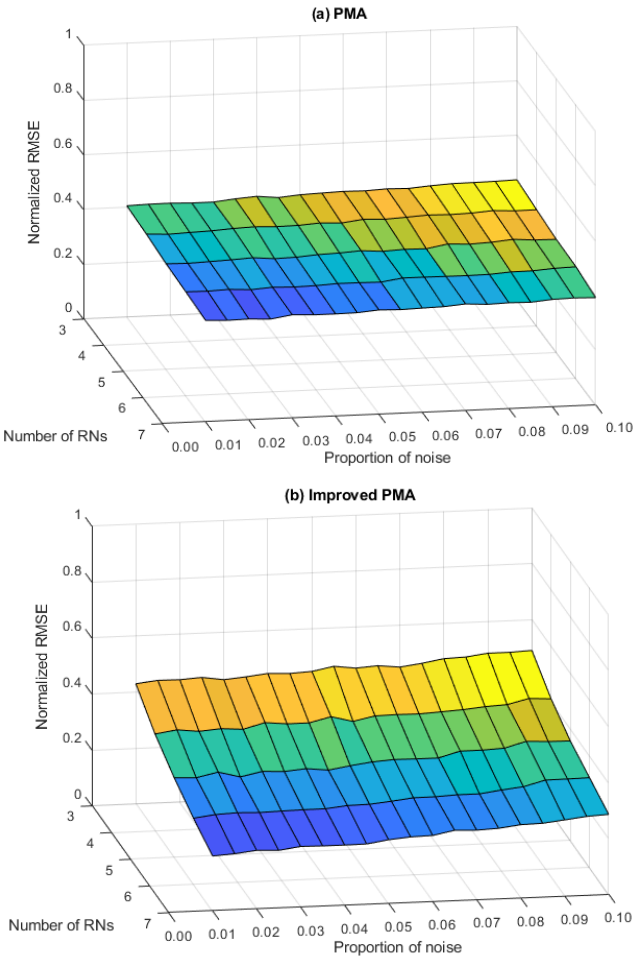

FIGURE 20. Normalized RMSE vs proportion of noise starting at 3 and up to 7 RNs for (a) PMA and (b) Improved PMA for the third case in a multi-hop network.

We can see in Figure 19(b) that there is a diminution of the normalized RMSE on the localization techniques presented as the number of RNs increases to 7 nodes. We can also see that the algorithm PMA displays a similar behavior regarding the normalized RMSE for 5 and 7 RNs.

According to Figure 20, we can see that the normalized RMSE of the algorithm PMA displays a steady performance in terms of the normalized RMSE varying the amount of RNs and noise level. In the case of the algorithm WMA, considering 3 RNs randomly arranged, we can notice that it shows very high error values; therefore, starting from 4 RNs, we get a more robust normalized RMSE value. When considering a network with 3 RNs randomly arranged, there is no guarantee of good NOI localization because the area [covered] by 3 RNs in some case can be very small, thus, we get high inaccuracy in the localization of the NOI. Figure 20(b) shows that the proposed algorithm Improved PMA displays a rugged behavior in terms of the normalized RMSE starting from 5 RNs, as we vary the proportion noise. Therefore, we may conclude that the performance of the proposed algorithm Improved PMA is affected by the geometry of the RNs, thus, we need at least 5 RNs randomly distributed to obtain an estimation of the NOI localization with little error variation.

In the three test cases previously described, we can see that the algorithm WMA displays better performance in regards to the Normalized RMSE than the others analyzed algorithms considering low proportion noise levels; whereas the algorithm PMA maintains a steady performance regarding the Normalized RMSE as we increase the number of RNs, therefore, the performance of this algorithm is not affected by the number of RNs. Thus, a network with 3RNs using solid triangular geometry is enough to obtain a good estimation of the NOI considering the algorithm PMA. In case 3, where the RNs are randomly distributed, the analyzed localization algorithms display a higher Normalized RMSE than that of cases 1 and 2. We can also see in this case that the localization algorithm WMA displays a better performance than the other analyzed algorithms as we increase the number of RNs, in the single-hop and multi-hop scenarios. Finally we can see that

for 5 RNs or more RNs in the network, the localization algorithm WMA displays greater sturdiness than the other analyzed algorithms.

VII. CONCLUSION

This paper evaluates the performance of localization algorithms regarding the normalized RMSE varying the proportion of noise and the number of RNs. By analyzing the obtained results, we learn that the algorithm MA presents a steady performance regarding the normalized RMSE considering at least 3 RNs with a solid triangular geometry and proportion noise. We also learn that the algorithm PMA displays a steady normalized RMSE varying the proportion noise and the number of RNs; hence, the performance of this algorithm is affected to a low extent by the noise environment and such performance regarding the normalized RMSE is not affected by the geometry of the RNs. However, the algorithm WMA displays a rugged performance regarding the normalized RMSE considering at least 5 RNs regardless of their geometry. This paper shows that the proposed algorithm Improved PMA presents a better performance than the other analyzed algorithms considering the single-hop and multi-hop scenarios. Our proposed algorithm Improved PMA considers the environment analysis due to the RSS and the mobility of the node of interest in the calculation of the correlation matrix that considers the variance of the separation distance between the node of interest and its respective RNs. We also consider a damping factor, which improves the convergence of the proposed algorithm Improved PMA. According to the results we obtained, our proposed algorithm Improved PMA, presents greater robustness than the algorithms MA and WMA in the single-hop and multi-hop scenarios.

REFERENCES

[1] V. Ramasamy, "Mobile wireless sensor networks: An overview," in *Insights and Innovations*. London, U.K.: IntechOpen, 2017.
[2] A. Abid, F. Khan, M. Hayat, and W. Khan, "Real-time object tracking in wireless sensor network," in *Proc. 10th Int. Conf. Elect. Electron. Eng.*, Bursa, Turkey, 2017, pp. 1103–1107.
[3] L. Chelouah, F. Semchedine, and L. Bouallouche-Medjkoune, "Localization protocols for mobile wireless sensor networks: A survey," *Comput. Electr. Eng.*, vol. 71, pp. 733–751, Oct. 2018.
[4] J. Al-Muhtadi, M. Qiang, K. Zeb, J. Chaudhry, K. Saleem, A. Derhab, M. A. Orgun, R. Shankaran, M. Imran, and M. Pasha, "A critical analysis of mobility management related issues of wireless sensor networks in cyber physical systems," *IEEE Access*, vol. 6, pp. 16363–16376, 2018.
[5] A. Paul and T. Sato, "Localization in wireless sensor networks: A survey on algorithms, measurement techniques, applications and challenges," *J. Sensor Actuator Netw.*, vol. 6, no. 4, p. 24, Oct. 2017.
[6] S. Durugkar and R. C. Poonia, "Optimum utilization of natural resources for home garden using wireless sensor networks," *J. Inf. Optim. Sci.*, vol. 38, no. 6, pp. 1077–1085, Oct. 2017.
[7] F. Deng, S. Guan, X. Yue, X. Gu, J. Chen, J. Lv, and J. Li, "Energy-based sound source localization with low power consumption in wireless sensor networks," *IEEE Trans. Ind. Electron.*, vol. 64, no. 6, pp. 4894–4902, Jun. 2017.
[8] Y.-W. Kuo, C.-L. Li, J.-H. Jhang, and S. Lin, "Design of a wireless sensor network-based IoT platform for wide area and heterogeneous applications," *IEEE Sensors J.*, vol. 18, no. 12, pp. 5187–5197, Jun. 2018.
[9] A. Gawanmeh and K. Saleem, "Introduction to the special issue on communication, computing, and networking in cyber-physical systems," *Scalable Comput., Pract. Exper.*, vol. 18, no. 4, Nov. 2017.
[10] K. Saleem, Z. Tan, and W. Buchanan, "Security for cyber-physical systems in healthcare," in *Health 4.0: How Virtualization and Big Data are Revolutionizing Healthcare*. Cham, Switzerland: Springer, 2017, pp. 233–251.
[11] A. Sajid, H. Abbas, and K. Saleem, "Cloud-assisted IoT-based SCADA systems security: A review of the state of the art and future challenges," *IEEE Access*, vol. 4, pp. 1375–1384, 2016.
[12] A. Coluccia and A. Fascista, "A review of advanced localization techniques for crowdsensing wireless sensor networks," *Sensors*, vol. 19, no. 5, p. 988, Feb. 2019.
[13] Z. Qiu, L. Wu, and P. Zhang, "An efficient localization method for mobile nodes in wireless sensor networks," *Int. J. Online Eng.*, vol. 13, no. 3, p. 160, Mar. 2017.
[14] G. S. Sara and D. Sridharan, "Routing in mobile wireless sensor network: A survey," *Telecommun. Syst.*, vol. 57, no. 1, pp. 51–79, Aug. 2013.
[15] A. Sayyed and L. B. Becker, "A survey on data collection in mobile wireless sensor networks (MWSNs)," in *Cooperative Robots and Sensor Networks*. New York, NY, USA: Springer, 2015, pp. 257–278.
[16] K. M. Awan, P. A. Shah, K. Iqbal, S. Gillani, W. Ahmad, and Y. Nam, "Underwater wireless sensor networks: A review of recent issues and challenges," *Wireless Commun. Mobile Comput.*, vol. 2019, pp. 1–20, Jan. 2019.
[17] R. M. Zuhairy and M. G. Al Zamil, "Energy-efficient load balancing in wireless sensor network: An application of multinomial regression analysis," *Int. J. Distrib. Sensor Netw.*, vol. 14, no. 3, Mar. 2018, Art. no. 155014771876464.
[18] A. Chizhov and A. Karakozov, "Wireless sensor networks for indoor search and rescue operations," *Int. J. Open Inf. Technol.*, vol. 2, pp. 1–4, Feb. 2017.
[19] M. Akter, M. O. Rahman, M. N. Islam, M. M. Hassan, A. Alsanad, and A. K. Sangaiah, "Energy-efficient tracking and localization of objects in wireless sensor networks," *IEEE Access*, vol. 6, pp. 17165–17177, 2018.
[20] C. Vargas-Rosales, D. Munoz-Rodriguez, R. Torres-Villegas, and E. Sanchez-Mendoza, "Vertex projection and maximum likelihood position location in reconfigurable networks," *Wireless Pers. Commun.*, vol. 96, no. 1, pp. 1245–1263, Apr. 2017.
[21] C. Vargas-Rosales, J. Mass-Sanchez, E. Ruiz-Ibarra, D. Torres-Roman, and A. Espinoza-Ruiz, "Performance evaluation of localization algorithms for WSNs," *Int. J. Distrib. Sensor Netw.*, vol. 11, no. 3, Jan. 2015, Art. no. 493930.
[22] J. Mass-Sanchez, E. Ruiz-Ibarra, A. Gonzalez-Sanchez, A. Espinoza-Ruiz, and J. Cortez-Gonzalez, "Factorial design analysis for localization algorithms," *Appl. Sci.*, vol. 8, no. 12, p. 2654, Dec. 2018.
[23] K. Zheng, H. Wang, H. Li, W. Xiang, L. Lei, J. Qiao, and X. Sherman Shen, "Energy-efficient localization and tracking of mobile devices in wireless sensor networks," *IEEE Trans. Veh. Technol.*, vol. 66, no. 3, pp. 2714–2726, Mar. 2017.
[24] H. Rashid and A. K. Turuk, "Dead reckoning localisation technique for mobile wireless sensor networks," *IET Wireless Sensor Syst.*, vol. 5, no. 2, pp. 87–96, Apr. 2015.
[25] H. Chen, F. Gao, M. Martins, P. Huang, and J. Liang, "Accurate and efficient node localization for mobile sensor networks," *Mobile Netw. Appl.*, vol. 18, no. 1, pp. 141–147, 2013.
[26] S.-J. Liu, R. Y. Chang, and F.-T. Chien, "Analysis and visualization of deep neural networks in device-free Wi-Fi indoor localization," *IEEE Access*, vol. 7, pp. 69379–69392, 2019.
[27] R. R. Roy, *Handbook of Mobile Ad Hoc Networks for Mobility Models*. New York, NY, USA: Springer, 2011, doi: 10.1007/978-1-4419-6050-4.
[28] T. Camp, J. Boleng, and V. Davies, "A survey of mobility models for ad hoc network research," *Wireless Commun. Mobile Comput.*, vol. 2, no. 5, pp. 483–502, 2002.
[29] S. P. Singh and S. C. Sharma, "Range free localization techniques in wireless sensor networks: A review," *Procedia Comput. Sci.*, vol. 57, pp. 7–16, Mar. 2015.
[30] W.-C. Lai, Y.-Y. Su, C.-M. Lee, S.-H. Fang, W.-J. Lin, X.-P. He, and K.-C. Feng, "A survey of secure fingerprinting localization in wireless local area networks," in *Proc. 12th Int. Conf. Mach. Learn. Cybern. (ICMLC)*., Jul. 2013, pp. 1413–1417.
[31] J. Mass-Sanchez, E. Ruiz-Ibarra, J. Cortez-González, A. Espinoza-Ruiz, and L. A. Castro, "Weighted hyperbolic DV-hop positioning node localization algorithm in WSNs," *Wireless Pers. Commun.*, vol. 96, no. 4, pp. 5011–5033, 2017.
[32] Y. I. Wu, "Multiple sources localization with WSN, eliminating the Direction-of-Arrival ambiguity symmetric with respect to the planar array," *IEEE Access*, vol. 6, pp. 46290–46296, 2018.

[33] D. Munoz, F. Bouchereau, C. Vargas, and R. Enriquez, *Position Location Techniques and Applications*. Amsterdam, The Netherlands: Elsevier, 2009.
[34] T. He, C. Huang, B. M. Blum, J. A. Stankovic, and T. Abdelzaher, "Range-free localization schemes for large scale sensor networks," in *Proc. 9th Annu. Int. Conf. Mobile Comput. Netw. (MobiCom)*, San Diego, CA, USA, 2003, pp. 81–95.
[35] E. M. García, A. Bermúdez, R. Casado, and F. J. Quiles, "Wireless sensor network localization using hexagonal intersection," in *Proc. IFIP Conf. Wireless Sensor Actor Netw.*, vol. 248, 2007, pp. 155–166.
[36] A. M. A. Abu Znaid, M. Y. I. Idris, A. W. Abdul Wahab, L. Khamis Qabajeh, and O. Adil Mahdi, "Sequential Monte Carlo localization methods in mobile wireless sensor networks: A review," *J. Sensors*, vol. 2017, pp. 1–19, Apr. 2017.
[37] S. Zhang, J. Cao, C. Li-Jun, and D. Chen, "Accurate and energy-efficient range-free localization for mobile sensor networks," *IEEE Trans. Mobile Comput.*, vol. 9, no. 6, pp. 897–910, Jun. 2010.
[38] S. H. Thimmaiah and G. Mahadevan, "Analysis of improved DV-distance algorithm for distributed localization in WSNs," *Int. J. Eng. Res. Develop.*, vol. 14, no. 2, pp. 16–20, 2018.
[39] A. H. Sayed, A. Tarighat, and N. Khajehnouri, "Network-based wireless location," *IEEE Signal Process. Magazine.*, vol. 22, no. 4, pp. 24–40, 2005.
[40] X. Ji and H. Zha, "Sensor positioning in wireless ad-hoc sensor networks using multidimensional scaling," in *Proc. IEEE 23rd Annu. Joint Conf. IEEE Comput. Commun. Soc. (INFOCOM)*, Mar. 2004, pp. 2652–2661.
[41] S. Zhang, J. Li, B. He, and J. Chen, "LSDV-Hop: Least squares based DV-hop localization algorithm for Wireless sensor networks," *J. Commun.*, vol. 11, pp. 243–248, Mar. 2016.
[42] P. Bergamo and G. Mazzini, "Localization in sensor networks with fading and mobility," in *Proc. 13th IEEE Int. Symp. Pers., Indoor Mobile Radio Commun.*, vol. 2, Sep. 2002, pp. 750–754.
[43] T. Watkins. *Bézout's Theorem*. Accessed: Jan. 2020. [Online]. Available: http://www.sjsu.edu/faculty/watkins/bezout.htm
[44] T. S. Rappaport, *Wireless Communications: Principles and Practice*, 2nd ed. Upper Saddle River, NJ, USA: Prentice-Hall, 2010.
[45] D. Huh and T. J. Sejnowski, "Gradient descent for spiking neural networks," in *Proc. 32nd Conf. Neural Inf. Process. Syst.*, 2017, pp. 1433–1443.
[46] Z. Yang and Y. Liu, "Quality of trilateration: Confidence-based iterative localization," *IEEE Trans. Parallel Distrib. Syst.*, vol. 21, no. 5, pp. 631–640, May 2010.

JOAQUIN MASS-SANCHEZ received the degree in electronics engineer from the Sonora Institute of Technology (ITSON), in 2011, and the M.Sc. degree from the Center for Advanced Research and Education, National Polytechnic Institute (CINVESTAV-IPN), Guadalajara, Mexico, in 2014. He is currently pursuing the Ph.D. degree with the Sonora Institute of Technology. His research interests include localization in wireless sensor networks, mobile ad hoc networks, mobility, stochastic modeling, digital signal processing applications, and digital communications.

CESAR VARGAS-ROSALES (Senior Member, IEEE) received the M.Sc. and Ph.D. degrees in electrical engineering from Louisiana State University, with a focus on communications and signal processing. He was the Director of the Ph.D. Program in information and communications technologies with the Tecnológico de Monterrey, Campus Monterrey, from 2012 to 2016, where he is currently the Leader of the Research Group on Telecommunications. He has coauthored the book *Position Location Techniques and Applications* (Academic Press/Elsevier). His research interests include personal communications, 5G, cognitive radio, MIMO systems, mobility, stochastic modeling, traffic modeling, intrusion/anomaly detection in networks, position location, interference, routing in reconfigurable networks, and optimum receiver design. He is also a member of the Mexican National Researchers System (SNI) Level II, the Academy of Engineering of Mexico, and the Mexican Academy of Sciences. He is the IEEE Communications Society Monterrey Chapter Chair and the Faculty Advisor of the IEEE-HKN Lambda-Rho Chapter. He was also the Technical Program Chair of the IEEE Wireless Communications and Networking (WCNC) Conference, in 2011. He is also an Associate Editor of IEEE Access journal.

ERICA RUIZ-IBARRA received the M.Sc. and Ph.D. degrees in electronic and telecommunication from CICESE, Mexico, in 2000 and 2010, respectively. She is currently an Electrical and Electronics Engineering Professor with the Sonora Institute of Technology. Her research interests include sensor networks, design and performance evaluation of routing protocol, digital communications, and human–computer interaction.

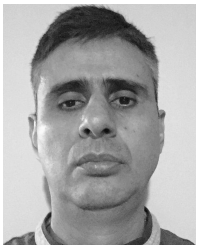

ARMANDO GARCIA-BERUMEN received the B.S. degree in electronic engineering from the Durango Institute of Technology, in 1995, the master's degree with emphasis on telecommunications from the Monterrey Institute of Technology and Higher Studies (ITESM), and the Ph.D. degree in information technology and telecommunication from Telecom SudParis (formerly the National Institute of Telecommunications) in Evry, France, in 2009. He has been a full-time Teacher with the Department of Electrical and Electronic Engineering, Sonora Institute of Technology (ITSON), since 1999. It has several publications in national and international congresses. His research interests are wireless networks, the IoT, and embedded systems.

ADOLFO ESPINOZA-RUIZ received the master's degree in computer sciences from the ITESM campus Estado de Mexico, in 2003. He is currently an Electrical and Electronics Engineering Professor with the Sonora Institute of Technology. His teaching and research interests include embedded systems, soft computing, and wireless sensor networks.